# Journal Pre-proof


Successful Formulation Window for the design of pharmaceutical tablets with required mechanical properties

P. Polak, I.C. Sinka, G.K. Reynolds, R.J. Roberts

PII: S0378-5173(23)01127-4
DOI: https://doi.org/10.1016/j.ijpharm.2023.123705
Reference: IJP 123705

To appear in: *International Journal of Pharmaceutics*

Received date : 10 October 2023
Accepted date : 11 December 2023

Please cite this article as: P. Polak, I.C. Sinka, G.K. Reynolds et al., Successful Formulation Window for the design of pharmaceutical tablets with required mechanical properties. *International Journal of Pharmaceutics* (2023), doi: https://doi.org/10.1016/j.ijpharm.2023.123705.

# Successful Formulation Window for the design of pharmaceutical tablets with required mechanical properties

P. Polak[a], I.C. Sinka[a,*], G.K. Reynolds[b], R.J. Roberts[b]

[a] *School of Engineering, University of Leicester, UK*
[b] *Oral Product Development, Pharmaceutical Technology and Development, Operations, AstraZeneca, Macclesfield, UK*

**Abstract**

Pharmaceutical tablet formulations combine the active ingredient with processing aids and functional components. This paper evaluates compressibility based predictive models for binary and ternary formulations to establish an acceptable range of tablet compression parameters that satisfy prescribed quality target criteria for tablets including minimum tablet strength and processing constraints such as maximum ejection stress and maximum compaction pressure. The concept of Successful Formulation Window (SFW) is introduced. A methodology is proposed to determine the SFW for a given formulation based on compaction simulator data collected for individual formulation components. The methodology is validated for binary and ternary mixtures and lubricated formulations. The SFW analysis was developed to support tablet formulation design to meet mechanical requirements.

*Keywords:* Successful Formulation Window, Tablet strength, Ejection stress, Compaction simulator, Lubrication

## 1. Introduction

The popularity of tablets as a drug delivery system stems from advantages including low cost, long term storage stability, good tolerance to temperature, efficient manufacturing and ease of use by patients. Tablet manufacturing is a unit operation where a bulk powder material is compacted in a die using two opposing compression punches until the compact satisfies prescribed dissolution/disintegration and mechanical requirements. Powder formulations include the active pharmaceutical ingredient (API) and excipients which are pharmacologically inactive substances such as binders, diluents, disintegrants, lubricants and other processing aids necessary to achieve the desired bioavailability of the drug and physico-mechanical properties of tablets. Excipients can make up a significant proportion of the volume of tablet formulations. Excipients are derived from various sources such as animal (e.g. gelatine, lactose, stearic acid, etc.), plant (arginates, cellulose, starches, sugar, etc.), mineral (e.g. calcium phosphate, silica, etc.) and synthetic (e.g. polysorbates, povidone, etc.). Further information of origin, source and functionality can be found in (Pifferi and Restani, 2003; Sheskey et al., 2020). Binders and diluents are used to add bulk, increase the strength of the tablets or improve flow properties (Arndt and Kleinebudde, 2018). Their rational selection in compositions influences the stability and bioavailability of the medicine (Reddy et al., 2013). Lubricants represent a particularly important class of pharmaceutical excipients which enable tablet manufacturing by reducing the friction between tooling and the powder material (Paul and Sun, 2018), thus reducing the compaction and ejection forces (Uzondu et al., 2018) or increase tablet brittleness (Paul and Sun, 2017a). However, the use of lubricants in formulations typically has a negative influence on tablet strength (Jarosz and Parrott, 1984; Miller and York, 1988) and tablet disintegration time (Shotton and Lewis, 1964). One of the most

*Corresponding authors
*Email address:* ics4@leicester.ac.uk (I.C. Sinka)

widely used lubricant in pharmaceutical tablet formulation is Magnesium Stearate (Miller and York, 1988). Lubricants may also prevent the adhesion of material to the punches (known as sticking) and minimize punch wear (Zuurman et al., 1999; Mitrevej and Augsburger, 1982). However, Magensium Stearate does not always prevent sticking (Roberts et al., 2004). Lubrication theory generally distinguishes two main types of lubrication (1) hydrodynamic or fluid lubrication, where the moving surfaces are separated by a layer of lubricant of a given viscosity, (2) boundary lubrication, where a thin film of lubricant separates the surfaces in contact influencing (a) friction, by supporting the interfacial load and (b) cohesion formed at particle-particle asperities or/and adhesion formed by particle-tooling asperities which penetrate the lubricant layer (Bowden and Tabor, 1967; Roblot-Treupel and Puisieux, 1986; Miller and York, 1988). Typical lubricants used in pharmaceutical formulations are boundary lubricants which are chemically inert, odourless and without taste (Wang et al., 2010).

Tablet manufacturing includes the tabletting operation and post-compaction processes such as coating (to protect from exposure to light, moisture and oxygen; to improve appearance, to mask taste or to control drug release), packaging, handling, storage and use. The formulation must be designed so that tablets meet a required set of mechanical properties to withstand the above-mentioned conditions. One of the key manufacturing requirements is tensile strength. The standard method to characterise the tensile strength of a tablet is the diametrical compression test described by (Fell and Newton, 1970). The test was first introduced by (Carneiro and Barcellos, 1953) as an indirect method to measure the tensile strength of rock and concrete. The analytical framework to determine the tensile stress under which the compact undergoes failure is based on a stress solution by H. R. Hertz in 1883 (Mellor and Hawkes, 1971) developed for a cylindrical disk compressed between two diametrically opposite platens. According to Hertz, the tensile strength of the materials is calculated as

$$\sigma_T = \frac{2F}{\pi D t} \tag{1}$$

where $\sigma_T$, $F$, $D$ and $t$ are tensile strength, break force, diameter and thickness of the tablet, respectively. It is intuitive to consider that by increasing the compaction force applied by the punches the density and strength of the resulting compact will increase accordingly.

Various tabletting related concepts are in use, e.g. the United States Pharmacopeia (USP40) issued a supplement in 2017 using following definitions:

- compressibility: solid volume fraction as a function of compaction pressure,
- compactability: tensile strength as a function of solid fraction,
- tabletability: tensile strength as a function of compaction pressure.

Compactability and tabletability relationships have been studied extensively (Balshin, 1949; Ryshkewitch, 1953; Higuchi et al., 1954; Shotton and Ganderton, 1961; Hasselman, 1969; Schiller, 1971; Leuenberger, 1982; Fleck, 1995; LaMarche et al., 2014; Persson and Alderborn, 2018) and empirical or semi-empirical relations were established. A common feature of these equations is that the compactability or tabletability are determined for a given powder mixture. Theories of tensile strength of powder compacts were proposed by (Rumpf, 1962; Smalley and Smalley, 1964) were the effects of particle size and interparticle forces were considered. There has been an increasing interest to describe and predict the tablet tensile strength of binary mixtures from individual component property contributions (Chan et al., 1983; Bangudu and Pilpel, 1984). The theory of Cheng (Cheng, 1968) accounts for particle size distribution, powder density and interparticle force. More recent research focussed on the rule of mixtures to predict tablet strength from the properties of individual powder constituents (Leuenberger, 1982; Kuentz, 1999; Kuentz and Leuenberger, 2000; Ramirez et al., 2004; Wu et al., 2005, 2006; Busignies et al., 2006; Michrafy et al., 2007; Etzler et al., 2011; Busignies et al., 2012; Juban et al., 2015; Capece et al., 2015; Reynolds et al., 2017; Radojevic and Zavaliangos, 2017).

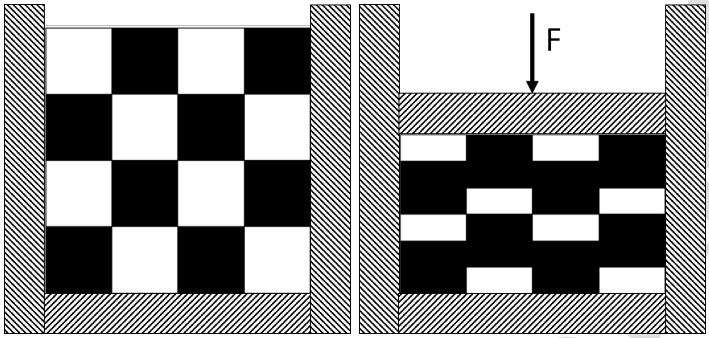


**Figure 1:** Mesoscopic representation of volume change of individual constituent at the same compaction pressure. Adapted from (Reynolds et al., 2017)

In this paper we extend the data set produced by (Reynolds et al., 2017) with experiments using lubricated mixtures. The methodology developed by (Reynolds et al., 2017) is adopted where the rules of mixture is based on the volume fraction of an individual component under the same compaction pressure, as illustrated in Figure 1. The data analysis methodology is extended to consider the ejection stress and the effect of lubricants. The key contribution of the paper is the concept of Successful Formulation Window (SFW) a predictive analysis tool that determines the porosity range and the compaction pressure range (window) needed to compress a given powder formulation into an acceptable tablet. The SFW addresses the mechanical aspects of formulation and tablet pressing and involves the following steps:

1. identify the critical quality attributes that describe the mechanical behaviour of the tablets,
2. for each individual powder material in the formulation characterise:
   (a) compressibility,
   (b) compactability,
   (c) ejection stress,
3. employ and verify the rules of mixtures to predict the compressibility, compactability and ejection stress of a mixture,
4. verify the methodology using experimental data for the formulation,
5. data visualization.

## 2. Mechanical quality attributes of tablets

The starting point to determine the SFW for a pharmaceutical formulation is represented by the following three criteria concerned with the mechanical quality attributes of tablets. First, the tablet material must have a minimum tensile strength to withstand post-compaction loading. Strength is related to bioavailability, e.g. it is possible to engineer high strength tablets, however, high strength may adversely affect disintegration time thus bioavailability after administration. Second, the maximum compression pressure (defined as the force applied to the compression tool divided by the cross-sectional area of the die) is limited as high stress leads to plastic yielding, brittle fracture, fatigue, and wear of the die and punches. Third, the ejection stress (defined as the ejection force divided by the area of tablet in contact with the die) must be limited in order to be able to eject tablets from the die. High ejection stresses are often responsible for defects such as capping and laminations. As described above, lubrication can be used to mitigate friction and thus reduce the ejection stress, however, admixing lubricants to tablet formulations typically affects

bioavailability in a negative manner (e.g. spreading hydrophobic lubricants over the surface of particles and granules reduces dissolution). The mechanical criteria required for a pharmaceutical tablet formulation are listed in Table 1 (Leane et al., 2015). Although in practice it is preferable that the ejection stress would be less then tensile stress.

**Table 1:** Formulation criteria - mechanical requirements for tablet design and manufacturing

| *Formulation criteria* | *Tablet strength* $\sigma_T^{Crit}$ $Pa \times 10^6$ | *Compaction pressure* $\sigma_C^{Crit}$ $Pa \times 10^6$ | *Ejection stress* $\sigma_{Ej}^{Crit}$ $Pa \times 10^6$ |
|---|---|---|---|
| Minimum | 2 | - | - |
| Maximum | - | 300 | 3 |

## 3. Models for compressibility, compactability and ejection stress

In this work we use the definitions of compressibility and compactability according to the United States Pharmacopoeia (USP40).

### *3.1. Compressibility*

Compressibility is defined as the volume reduction (densification) under the applied compaction pressure. Various empirical relationships have been proposed to describe the compressibility of powder materials undergoing compaction. These equations must satisfy the principle of dimensional homogeneity (Cardei, 2017). The evaluation of parameters and benchmarking by (Denny, 2002) for the Heckel (Heckel, 1961a) and Kawakita (Kawakita and Lüdde, 1971) equations have established a complete correspondence between physical/mechanical properties and densification behaviour. The importance of anisotropy and variation of Poisson's ratio was highlighted (Denny, 2002). The Gurnham equation (Gurnham and Masson, 1946) has been used by (Zhao et al., 2006) for excipients such as Microcrystalline cellulose, Corn starch, Lactose monohydrate, and dibasic calcium phosphate. It was concluded that the fitting parameter $d$ (introduced in Table 2) is a representative compressibility property. The influence of varying compaction pressure on the plastic energy, elasticity, particle yield strength, strain hardening and applied pressures on the Heckel parameter where studied by (Patel et al., 2010). Heckel fitting parameter $K$ (reciprocal of the yield strength) was found to be strongly dependent on compaction pressure. (Mahmoodi et al., 2013) investigated the suitability of an effective medium equation to describe the compaction pressure as a function of yield stress of the particles and powder bed height. A strong correlation between effective medium equation parameter and Heckel parameter $1/K$ was observed. In addition to the equation of Heckel Kawakita and Adams, the derivation of the yield stress parameter of a granule was investigated by (Persson et al., 2016). Paul and Sun (Paul and Sun, 2017b) concluded that the Kuentz-Leuenberger compressibility equation (Leuenberger, 1982; Kuentz and Leuenberger, 2000) can be used to characterise plasticity alongside to the Heckel, Kawakita and Walker equations (Walker, 1923).

The compressibility equations used in the current study are listed in Table 2. Relative density (RD) represents the solid volume fraction (equal to 1-porosity) and is used as a variable describing the state of densification of a powder. Compressibility functions are expressed in the form $RD = f(\sigma_C)$ or $\sigma_C = f^{-1}(RD)$.

**Table 2:** Compressibility equations

| *Name and Reference* | *Equation* | *No.* | *Parameters* |
|---|---|---|---|
| Heckel<br>(Heckel, 1961b) | $RD = 1 - exp(-A - K\,\sigma_C)$ | (1) | $A$ - fitting parameter<br>$K = \frac{1}{3\sigma_y}$<br>$\sigma_y$ - yield strength |
| Kawakita<br>(Kawakita and Lüdde, 1971) | $RD = \frac{RD_0\,(1+\sigma_C\,b)}{\sigma_C\,b\,(1-a)+1}$ | (2) | $RD_0$ - initial relative density<br>$a, b$ - fitting parameters |
| Kuentz-Leuenberger<br>(Kuentz and Leuenberger, 1999) | $\sigma_C = \frac{1}{C}\,[RD_c - RD - ...$<br>$(1 - RD_c)\,log(\frac{1-RD}{1-RD_c}]$ | (3) | $\frac{1}{C}$ - plasticity parameter<br>$RD_c$ - relative density at which compact starts to form |
| Modified Gurnham<br>(Reynolds et al., 2017) | $RD = \frac{log(\frac{\sigma_C}{\overline{\sigma}_C})}{d} + 1$ | (4) | $\overline{\sigma}_C$ - compaction pressure required to achieve $RD = 1$<br>$d$ - fitting parameter |

### *3.2. Compactability*

As powder is densified into a tablet the tensile strength of the material increases with increasing compaction pressure until a maximum of surface bonding area between particles is achieved (Kuentz and Leuenberger, 2000). The compactability relationships listed in Table 3 were used to interpolate and extrapolate the strength of the compact where the relative densities were obtained from the compressiblity equations for the single powder components. The empirical Ryshkewitch-Duckworth (Ryshkewitch, 1953) relationship developed for porosity dependent tensile strength of porous metal materials has been widely used for strength estimation of pharmaceutical tablets (Tye et al., 2005; Wu et al., 2005, 2006; Etzler et al., 2011; Reynolds et al., 2017). This relationship does not describe well the measured strength of compacts with low relative densities, however, this disadvantage can be overcome by the 3 parameter power law equation proposed in Table 3.

**Table 3:** Compactability equations in form of $\sigma_T = h(RD)$

| *Name and Reference* | *Equation* | *No.* | *Parameters* |
|---|---|---|---|
| Ryshkewitch-Duckworth<br>(Ryshkewitch, 1953) | $\sigma_T = \overline{\sigma}_T\,exp[e(RD-1)]$ | (5) | $e$ - bonding capacity<br>$\overline{\sigma}_T$ - Strength at $RD = 1$ |
| 3 par. Power law<br>(Garner et al., 2015)<br>(Al-Sabbagh et al., 2018) | $\sigma_T = c\,(RD - RD_0)^n$ | (6) | $c, n$ - fitting parameters<br>$RD_0$ - initial relative density |

### *3.3. Ejection model*

Die compaction can be divided into four main stages: (i) compaction (or application of load), (ii) dwell time (maintaining the maximum compaction pressure for a given time), (iii) unloading (removal of the applied load by the punches) and (iv) ejection of the tablet from the die using the lower punch. The ejection force is the maximum force applied by the lower punch during the ejection stage and is an indicator of

friction between tooling and tablet and/or residual die wall stress, which is applied to the tablet by elastic unloading of the die after the removal of the axial load at the end of stage (iii). In practice a small amount of lubricant is added to formulations to reduce friction and thus the ejection force. To determine ejection stress an empirical exponential relation is proposed (Equation (7)). The form of Equation (7) does not allow ejection stress to gain negative values as $RD \rightarrow RD_0$.

$$\sigma_{Ej} = exp[\beta + \alpha(RD - RD_0)] \tag{7}$$

where $\beta$ and $\alpha$ are fitting parameters and $RD_0$ is initial relative density.

### *3.4. Rules of mixtures*

A particle in a powder bed undergoes elastic and plastic deformation under the load applied by the punches during compaction. The macroscopic deformation of the powder bed, described by empirical compressibility relations such as those presented in Table 2, includes the contribution from each individual particle. To determine the compaction behaviour of binary, ternary and lubricated mixtures, the volume was assumed as the additive property, Equation (8).

$$V_{mix} = \sum_{n=1}^{\infty} V_i \tag{8}$$

where $V_{mix}$ and $V_i$ represents the volume of the mixture and of an individual component respectively and $n$ denotes the number of constituents in the mixture. Knowing the volume fraction of each constituent in Equation (9) the relative density of mixture is obtained by arithmetic mean of volumetric proportions of the constituents Equation (10). This approach provides an excellent agreement with experimental results (Busignies et al., 2012; Reynolds et al., 2017).

$$\zeta_{f_i} = \frac{\frac{m_{f_i}}{RD(\sigma_C)_i\, \rho_{true_i}}}{\sum_{n=1}^{\infty} \frac{m_{f_n}}{RD(\sigma_C)_n\, \rho_{true_n}}} \tag{9}$$

$$RD(\sigma_C)_{mix} = \sum_{n=1}^{\infty} \zeta_{f_i} RD(\sigma_C)_i \tag{10}$$

where $\zeta_{f_i}$, $m_{f_i}$, $RD_i$ are volume fraction, mass fraction and relative density of component $i$, respectively and $n$ is the number of components. Compactability is a property related to the surface bonding between particles in contact thus to the surface free energy of individual components. Applying Berthelot's rule (geometric mean), the tablet strength is extended for an assembly of particles as explained by (Etzler et al., 2011). Assuming similar particle size for the individual components, the strength of the mixture can be expressed by Equation (11) which represents a material property weighted via volumetric contribution of individual constituents. The same approach is applied to predict the ejection stress of the mixture. In addition to Berthelot's rule, two other Pythagorean means including the arithmetic mean (Equation (12)) and the harmonic mean (Equation (13)) weighted by volume fraction are used to evaluate their suitability to describe the experimental data below.

$$\psi_{Gmix} = \prod \psi(RD(\sigma_C)_i)_i^{\zeta_{f_i}} \tag{11}$$

$$\psi_{Amix} = \sum_{n=1}^{\infty} \psi(RD(\sigma_C)_i)_i\, \zeta_{f_i} \tag{12}$$

$$\psi_{Hmix} = \sum_{n=1}^{\infty} \left( \frac{\zeta_{f_i}}{\psi(RD(\sigma_C)_i)_i} \right)^{-1} \tag{13}$$

where $\psi_{G_{mix}}$, $\psi_{A_{mix}}$, $\psi_{H_{mix}}$ and $\psi_i$ are the predicted property of the mixture using geometric, arithmetic or harmonic averaging and measured property of the components, respectively.

## 4. Materials

The materials considered in this work are common pharmaceutical excipients used in tablet formulations: Microcrystalline cellulose, Calcium Phosphate, Mannitol and Magnesium Stearate (a lubricant). The materials were characterised as single components powders and mixtures. Information of grades, manufacturer and the composition of the formulations studied is presented in Table 4. The physical properties of the powders, including average particle size, specific surface area, bulk density and true density are presented in Table 5.

**Microcrystalline cellulose** (MCC) is described as a soft, ductile material with high compressibility (Rowe and Roberts, 1995), which undergoes large plastic deformation under pressure without showing brittleness. As plastic deformation takes place the contact areas between particles increases which leads to increased interparticle bonding (compactability). MCC exhibits time dependent behaviour (viscoelasticity) (Doelker, 1993; Bolhuis and Anthony Armstrong, 2006) and it is highly hygroscopic. Due to plastic deformation and low brittleness the particles do not fracture during loading and therefore no new surfaces are created which can lead to lubrication sensitivity (Bos et al., 1991; Zuurman et al., 1999; Hoag et al., 2008; Wang et al., 2010). MCC has a low coefficient of friction and low die wall residual stress compared to Mannitol (Doelker, 1993; Doelker and Massuelle, 2004) which lowers its requirements for lubrication. Detailed information about critical material attributes of MCC applied in direct compaction (DC) can be found in a review paper (Thoorens et al., 2014).

**Mannitol** is commonly used as a diluent in tablet formulations and behaves similarly to other sugars such as lactose or sucrose. Mannitol undergoes fragmentation under loading, however, also shows plastic deformation (Reynolds et al., 2017), which leads to high compactability. As a result of fragmentation Mannitol is less sensitive to lubrication than MCC. However, Mannitol has a higher coefficient of friction, therefore a lubricant is normally added to the formulation. Mannitol is non-hygroscopic and has good chemical stability.

**DiCalcium phosphate** (DCPA, ATAB) is typically used in nutritional health and food industry as a source of calcium and behaves similar to a ceramic powder. DCPA is a brittle material and fragments under pressure (Rowe and Roberts, 1995). Dicalcium phospate is less sensitive to lubrication due to a high particle fragmentation because new clean surfaces are created which are not exposed to lubricant. However, the addition of lubricant decreases flowability and compactability(Hwang and Peck, 2001).

Scanning electron microscopy (SEM) images of bulk powder of MCC, Mann and ATAB are shown in Figure 2.

**Mixtures and lubricated powders**. The binary and ternary mixtures of pure excipients are labelled using the mass fraction of the individual components (see Table 4). In addition, two batches of Mannitol lubricated with Magnesium stearate with mass fractions of 0.5% and 1% were characterized. The grade and manufacturer of the Magnesium stearate are listed in Table 4 and the physical properties are presented in Table 5.

**Magnesium stearate** (MgSt) is a boundary lubricant, categorized as a metallic salt of fatty acids with low melting point and good chemical stability. However due to the manufacturing process Magnesium stearate presents various impurities that can cause incompatibility with APIs. Due to its non-polar molecular structure it is insoluble in water.

**Table 4:** Grade and source of pure powder materials

| *Excipients* | *Abbreviated name* | *Grade* | *Manufacturer* | *Mass fraction (%)* |
|---|---|---|---|---|
| Microcrystalline cellulose | MCC102 | Avicel Ph102 | FMC Biopolymer, Ireland | - |
| Mannitol | Mann | Pearlitol SD200 | Roquette, France | - |
| DiCalcium Phosphate | ATAB | ATAB | Univar Innophos, USA | - |
| *Lubricant* | | | | |
| Magnesium Stearate | MgSt | MgSt MF2-V | Peter Greven | - |
| *Binary mixtures* | | | | |
| MCC102+Mann | M12_51/49 | - | - | 51:49 |
| MCC102+ATAB | M13_35/65 | - | - | 35:65 |
| Mann+ATAB | M23_34/66 | - | - | 34:66 |
| *Ternary mixtures* | | | | |
| MCC102+Mann+ATAB | M123_26/25/48 | - | - | 26:25:48 |
| MCC102+Mann+ATAB | M123_15/58/27 | - | - | 15:58:27 |
| MCC102+Mann+ATAB | M123_11/10/79 | - | - | 11:10:79 |
| MCC102+Mann+ATAB | M123_59/14/27 | - | - | 59:14:27 |
| *Lubricated material* | | | | |
| Mann+MgSt | Mann_05% | - | - | 99.5:0.5 |
| Mann+MgSt | Mann_1% | - | - | 99:1 |

**Table 5:** Physical properties of powder

| *Abbreviated name* | *Average particle size* $\times 10^{-4} m$ | *Specific surface area* $(m^2/kg) \times 10^{-3}$ | *Bulk density* $kg/m^3$ | *True density* $kg/m^3$ |
|---|---|---|---|---|
| MCC102 | 0.2 - 2 | 1.3 | 311.0 | 1559.9 |
| Mann | 1.5 - 2 | 15 | 488.0 | 1468.7 |
| ATAB | 2 - 3 | 0.38 | 725.0 | 2829.8 |
| MgSt | 0.04 - 0.1 | 5 | 159.0 | 1092.0 |

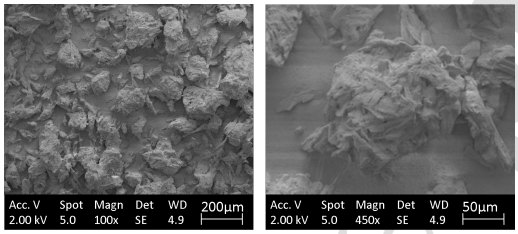


**(a)** MCC102

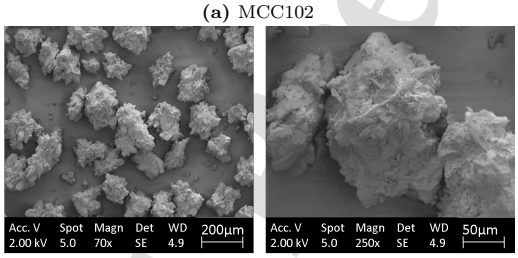


**(b)** Mann

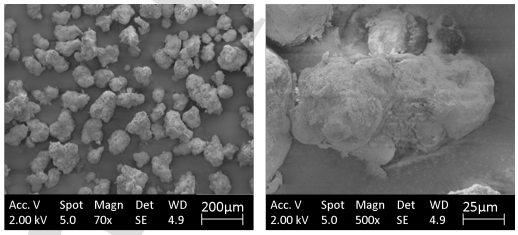


**(c)** ATAB

**Figure 2:** SEM images of powder materials and particle details (right)

## 5. Experimental methods

The experimental methods used to manufacture and characterise the lubricated powders follow the procedure described by Reynolds (Reynolds et al., 2017) which is summarised below for reasons of completeness and to highlight any differences in equipment and procedures given that in the current work lubrication is performed under different conditions.

### *5.1. Preparation of lubricated powder materials*

Lubricated Mannitol mixtures (Table 4) were prepared using a Turbula mixer T2F (Willy A. Bachofen, Switzerland) operated at 30 $rpm$ for 80 $sec$. The mixing time was chosen according to the studies of (Kikuta and Kitamori, 1994) which show that mixing affects compact strength, ejection force and disintegration time. It is important to note that MgSt was added through a sieve as lubricants tend to agglomerate affecting the material distribution in the mixture; such practices are common in pharmaceutical manufacturing.

The bulk and true density of the powder were obtained using the rules of mixtures based on volume fraction (Busignies et al., 2012; Reynolds et al., 2017) using Equations (9) and (10) and relative density $RD$ is calculated as:

$$RD = \frac{\rho}{\rho_{true}} \tag{14}$$

where $\rho$ and $\rho_{true}$ are current density of the powder and true density of the constituents, respectively. The initial relative density of the bulk powder state is $\rho = \rho_{bulk}$. The bulk and true density of pure materials were measured using a helium gas displacement pycnometer (AccuPyc II 1340, Micromeritics) with a 3.5$cm^3$ cup (Reynolds et al., 2017) and the results are presented in Table 5.

### *5.2. Compaction*

Compaction was carried out using a compaction simulator ESH (Phoenix, Rubery Owen, Telford, England) equipped with a 10 $mm$ diameter die instrumented with radial stress sensors tooled with flat faced punches, Figure 3. In order to reduce the effect of friction between the powder and tooling, the surfaces of punches and die were lubricated using MgSt, (Mallinckrodt Pharmaceuticals, Ireland) suspended in acetone. Once applied, the acetone was allowed to evaporate before use. The powder material was placed on the die table and introduced manually into the die cavity using a scraper to ensure that the die is completely filled before compaction. The compaction, unloading and ejection rates are listed in Table 6. The testing system records the compaction and ejection forces. Tablet dimensions (diameter $D$, height $t$) and weight $m$ were measured approx. 3 $min$ after ejection from the die and the relative density is calculated as:

$$RD = \frac{\rho}{\rho_{true}} = \frac{4m}{\pi D^2\, t\, \rho_{true}} \tag{15}$$

### *5.3. Ejection stress*

At the beginning of the ejection stage the tablet is stationary in the die, hence the force required to eject the tablet must overcome the static friction between the compact and die wall. After the tablet is in motion kinetic (dynamic or sliding) friction occurs. Therefore, the ejection profile includes static and kinetic ejection forces. The importance of the static friction during ejection and the kinetic friction during compaction is discussed by (Brewin et al., 2007) noting that friction can also be reduced by increasing the hardness of the tool material. The ejection stress of the is determined by measuring the ejection force $F_{Ej}$ of a flat faced tablet of diameter $D$ and thickness $t$, Equation (16):

$$\sigma_{Ej} = \frac{F_{Ej}}{\pi D t} \tag{16}$$

In the following analysis the static ejection force is obtained by the direct approach.

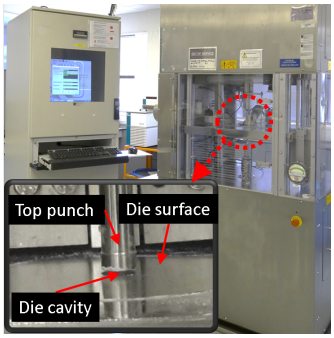


**Figure 3:** Compaction simulator. Detail: die instrumented with radial stress sensors

### *5.4. Tablet strength*

A set of tablets were compressed to different densities using a hydraulic testing machine, manufactured by MTS, using a 12.5 $mm$ diameter die, and flat faced tooling as illustrated in Figure 4. The ratio of $t/D \leq 0.25$ was chosen according to the studies of (Doremus et al., 2001). The compaction conditions are listed in Table 6 and the relative density of compacts were obtained using Equation (15). The tablet strength was measured using the diametrical compression test (Fell and Newton, 1970). A typical tensile failure pattern of the tablet is illustrated in Figure 5. The tensile strength of the tablet was calculated using Equation (1).

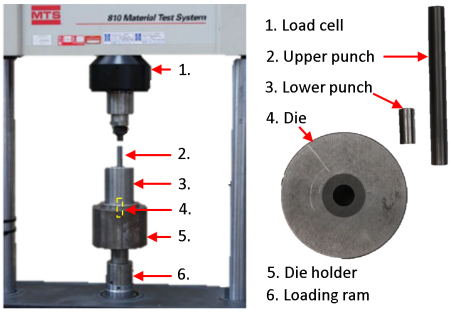


**Figure 4:** Cylindrical compact manufacturing set-up apparatus and tooling

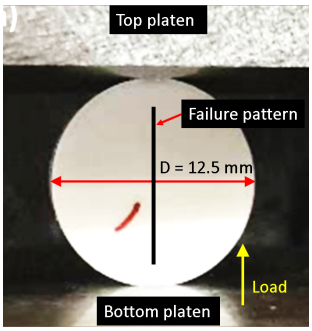


**Figure 5:** Diametrical compression test set up

**Table 6:** Experimental conditions and specimen characteristics (D-diameter, $t$-tablet thickness)

| *Experiment* | *Aspect ratio* | *Compaction* | | | *Diametrical Compression* |
|---|---|---|---|---|---|
| | $t/D$ $(-)$ | *Loading rate* $(mm \times min^{-1})$ | *Unloading rate* $(mm \times min^{-1})$ | *Ejection rate* $(mm \times min^{-1})$ | *Loading rate* $(mm \times min^{-1})$ |
| Diametrical compression | $\leq 0.25$ | 10 | 1 | $< 10$ | 1 |
| Compaction simulator | – | 10 | 10 | 10 | 1 |

## 6. Experimental data analysis

In this section we analyse the experimental data for single excipients and binary and ternary mixtures reported by Reynolds (Reynolds et al., 2017) and extend the analysis to ejection behaviour. The SFW (Successful Formulation Window) concept is put forward in Section 7 and lubricated mixture results are presented in Section 8. The compressibility equations (Table 2), compactability equations (Table 3) and ejection stress Equation (7) were fitted using non-linear least square solver build into the numerical computing language platform MATLAB version 2016 and higher.

### *6.1. Compressibility*

The four compressibility equations listed in Table 2 were used to fit the experimental data for pure excipients and mixtures. The fitting parameters together with the coefficient of determination ($R^2$) and 95% confidence interval ($Ci$) are listed in Table 7. A comparison of data and compressibility models is presented in Table 7, where the binary and ternary mixtures are separated for clarity in Figures 6a and 6b, respectively. The coefficient of determination $R^2$ presented in Table 7 show that all four models predicts well the densification behaviour within the studied compaction pressure range.

**Table 7:** Parameters of compressibility equations and errors

| *Material* | *modified Gurnham* | | | | | *Kawakita-Lude* | | | | |
|---|---|---|---|---|---|---|---|---|---|---|
| | $\overline{\sigma}_C$ $(MPa)$ | $\pm\, Ci$ $(MPa)$ | $d$ $(-)$ | $\pm\, Ci$ $(-)$ | $R^2$ $(-)$ | $a$ $(-)$ | $\pm\, Ci$ $(-)$ | $1/b$ $(MPa)$ | $\pm\, Ci$ $(MPa)$ | $R^2$ $(-)$ |
| MCC102 | 306.00 | 43.80 | 6.94 | 0.76 | 0.97 | 0.81 | 0.00 | 5.62 | 0.35 | 0.99 |
| Mann | 517.31 | 70.81 | 8.66 | 0.92 | 0.98 | 0.69 | 0.01 | 11.96 | 2.14 | 0.94 |
| ATAB | 10191.26 | 2632.90 | 10.70 | 0.68 | 0.99 | 0.67 | 0.01 | 19.14 | 3.09 | 0.95 |
| M12_51/49 | 397.23 | 28.57 | 8.19 | 0.50 | 0.99 | 0.77 | 0.00 | 8.01 | 0.41 | 0.99 |
| M13_35/65 | 1655.36 | 246.43 | 8.76 | 0.53 | 0.99 | 0.75 | 0.00 | 10.91 | 0.96 | 0.98 |
| M23_34/66 | 2494.60 | 261.94 | 10.07 | 0.37 | 1.00 | 0.68 | 0.01 | 13.38 | 1.99 | 0.95 |
| M123_26/25/48 | 1125.99 | 188.55 | 8.27 | 0.67 | 0.98 | 0.74 | 0.01 | 12.22 | 1.92 | 0.95 |
| M123_15/58/27 | 867.94 | 74.85 | 9.11 | 0.48 | 0.99 | 0.72 | 0.01 | 12.00 | 1.79 | 0.96 |
| M123_11/10/79 | 3039.41 | 769.59 | 9.56 | 0.80 | 0.98 | 0.71 | 0.01 | 13.87 | 2.58 | 0.92 |
| M123_59/14/27 | 721.85 | 99.11 | 8.42 | 0.69 | 0.98 | 0.78 | 0.00 | 8.30 | 0.80 | 0.98 |
| | *Kuentz-Leuenberger* | | | | | *Heckel* | | | | |
| | $1/C$ $(MPa)$ | $\pm\, Ci$ $(MPa)$ | $RD_c$ $(-)$ | $\pm\, Ci$ $(-)$ | $R^2$ $(-)$ | $1/K$ $(MPa)$ | $\pm\, Ci$ $(MPa)$ | $A$ $(-)$ | $\pm\, Ci$ $(-)$ | $R^2$ $(-)$ |
| MCC102 | 177.58 | 54.49 | 0.74 | 0.13 | 0.97 | 112.07 | 11.43 | 0.93 | 0.12 | 0.97 |
| Mann | 318.29 | 90.26 | 0.64 | 0.10 | 0.98 | 174.48 | 14.07 | 1.07 | 0.10 | 0.98 |
| ATAB | 3179.18 | 210.69 | 0.61 | 0.01 | 1.00 | 793.52 | 38.23 | 0.72 | 0.02 | 0.99 |
| M12_51/49 | 78.62 | 46.84 | 1.25 | 0.54 | 0.93 | 101.79 | 12.99 | 0.74 | 0.31 | 0.94 |
| M13_35/65 | 1405.93 | 296.36 | 0.55 | 0.04 | 0.98 | 429.90 | 47.87 | 0.90 | 0.07 | 0.95 |
| M23_34/66 | 1687.73 | 80.60 | 0.54 | 0.01 | 1.00 | 480.77 | 29.53 | 0.92 | 0.03 | 0.99 |
| M123_26/25/48 | 873.07 | 192.15 | 0.59 | 0.05 | 0.98 | 333.91 | 33.81 | 0.93 | 0.08 | 0.97 |
| M123_15/58/27 | 597.95 | 130.88 | 0.59 | 0.07 | 0.98 | 275.15 | 14.52 | 1.06 | 0.05 | 0.99 |
| M123_11/10/79 | 1581.60 | 181.45 | 0.60 | 0.02 | 0.99 | 510.08 | 25.17 | 0.82 | 0.02 | 0.99 |
| M123_59/14/27 | 697.10 | 227.69 | 0.53 | 0.08 | 0.96 | 265.00 | 34.18 | 1.08 | 0.12 | 0.94 |

The parameters of the mixtures were also calculated using arithmetic, geometric and harmonic means of single components based on volume fractions. Figure 6c and Figure 6d present the data for binary and ternary mixtures, respectively. For design of SFWs, the arithmetic mean based modified Gurnham compressibility model is used based on lower $R^2$ value.

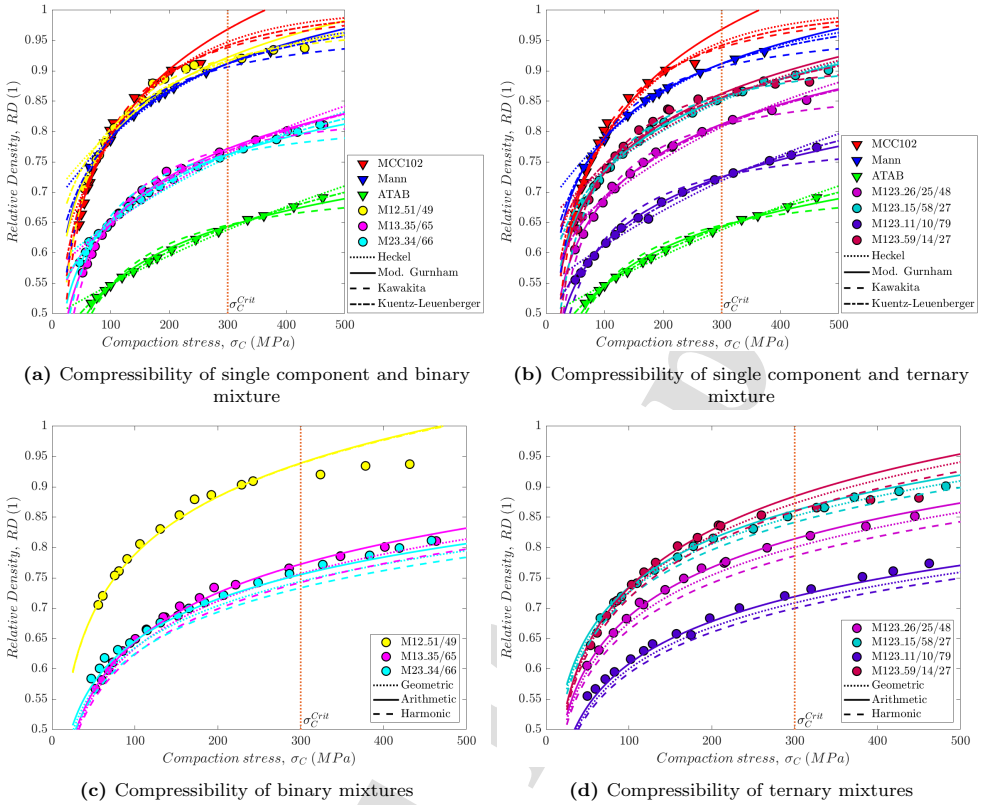


**(a)** Compressibility of single component and binary mixture

**(b)** Compressibility of single component and ternary mixture

**(c)** Compressibility of binary mixtures

**(d)** Compressibility of ternary mixtures

**Figure 6:** Compressibility

### *6.2. Compactability*

Tablet strength data for the single components and for mixtures are fitted using the two compactability equations in Table 2. The coefficient of determination $R^2$ and 95% confidence interval ($Ci$) are shown in Table 8. It can be concluded that both compactability models provide a good fit in the higher relative density range, however the 3 parameter power law model covers the lower relative densities better than the Ryshkewitch-Duckworth model which is exponential, as illustrated on Figure 7a and Figure 7b, although overall difference between two expression is relatively small. The strength of tablets consisting of binary and ternary mixtures is presented on Figure 7c and Figure 7d, respectively. In addition to Berthelot's rule (geometric mean), the arithmetic and harmonic means of tablet strength were determined. It can be observed that choice of mean rule is important for compactability. A quantitative evaluation of averaging rules is presented in Section 7.3.

**Table 8:** Parameters of compactability equations and errors

| *Material* | *Ryshkewitch-Duckworth* | | | | | *3 par. Power law* | | | | |
|---|---|---|---|---|---|---|---|---|---|---|
| | $\overline{\sigma}_{Dia}$ $(MPa)$ | $\pm Ci$ $(MPa)$ | $e$ $(-)$ | $\pm Ci$ $(-)$ | $R^2$ $(-)$ | $c$ $(MPa)$ | $\pm Ci$ $(MPa)$ | $n$ $(-)$ | $\pm Ci$ $(-)$ | $R^2$ $(-)$ |
| MCC102 | 15.39 | 1.60 | 6.47 | 0.84 | 0.97 | 35.84 | 6.87 | 4.16 | 0.50 | 0.97 |
| Mann | 9.61 | 1.42 | 10.25 | 1.69 | 0.96 | 81.45 | 37.52 | 5.95 | 0.93 | 0.97 |
| ATAB | 264.43 | 140.13 | 13.06 | 1.70 | 0.97 | 373.62 | 190.92 | 5.36 | 0.62 | 0.98 |
| M12_51/49 | 8.57 | 0.62 | 7.45 | 0.97 | 0.97 | 32.37 | 6.63 | 4.87 | 0.57 | 0.98 |
| M13_35/65 | 48.09 | 10.32 | 10.02 | 1.10 | 0.97 | 114.90 | 38.26 | 5.22 | 0.61 | 0.97 |
| M23_34/66 | 73.65 | 12.47 | 13.72 | 0.89 | 0.99 | 407.24 | 108.00 | 6.87 | 0.42 | 0.99 |
| M123_26/25/48 | 25.03 | 4.20 | 9.54 | 1.03 | 0.98 | 82.69 | 26.11 | 5.21 | 0.60 | 0.98 |
| M123_15/58/27 | 14.00 | 2.34 | 9.47 | 1.54 | 0.96 | 73.74 | 28.91 | 5.54 | 0.83 | 0.97 |
| M123_11/10/79 | 54.44 | 13.27 | 10.73 | 1.09 | 0.98 | 133.78 | 36.70 | 5.17 | 0.43 | 0.99 |
| M123_59/14/27 | 16.95 | 3.07 | 7.68 | 1.42 | 0.94 | 42.09 | 15.60 | 4.39 | 0.87 | 0.94 |

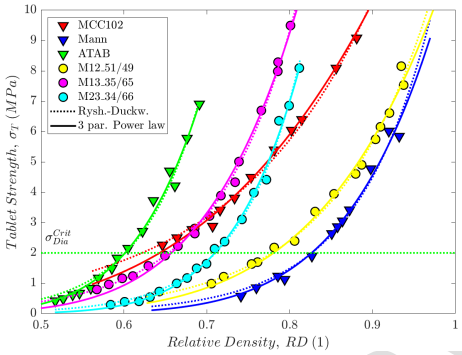


**(a)** Tablet strength vs. relative density of single component and binary mixture

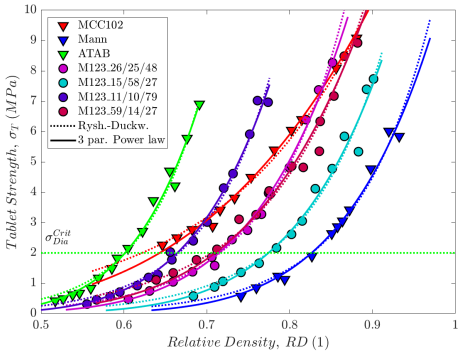


**(b)** Tablet strength vs. relative density of single component and ternary mixture

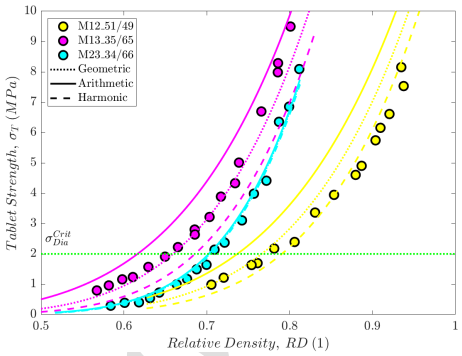


**(c)** Tablet strength vs. relative density of binary mixtures

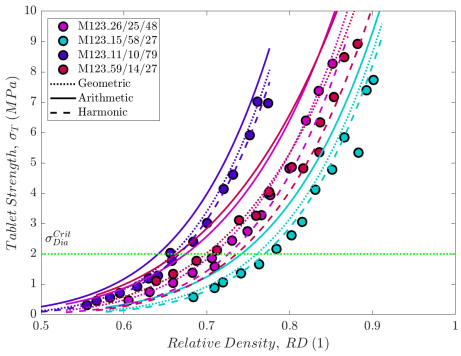


**(d)** Tablet strength vs. relative density of ternary mixtures

**Figure 7:** Compactability

### 6.3. Ejection stress

The ejection stress data obtained experimentally, presented in Figure 8, were fitted with Equation (7). The fitting parameters together with the coefficient of determination ($R^2$) and 95% confidence interval ($Ci$) are listed in Table 9. Except for pure MCC102 the ejection stress increase exponentially for all single materials and mixtures characterised in this work. The coefficient of determination of MCC102 is relatively low as the ejection stress does not change with increase of tablet relative density up to 0.85 above which the ejection stress decreases. The exponential ejection model does not adequately describe this experimental observation, as seen on Figure 8a where a graphical comparison of ejection model for pure excipients (line) with experimental data is plotted. The ejection stress of mixtures is influenced by the brittle constituent (Mann). It is interesting to note that M12_51/49 presents lower ejection stress than its individual components (MCC102 and Mann) at relative densities below 0.85. Figures 8c and 8d presents the ejection for binary and ternary mixtures, respectively, calculated using geometrical mean, arithmetic and harmonic means.

**Table 9:** Parameters of ejection model and errors

| *Material* | $\alpha$ | $\pm Ci$ | $\beta$ | $\pm Ci$ | $R^2$ |
|---|---|---|---|---|---|
| | $(Pa)$ | $(Pa)$ | $(Pa)$ | $(Pa)$ | $(-)$ |
| MCC102 | -2.40 | 1.24 | 15.04 | 0.79 | 0.60 |
| Mann | 9.54 | 1.82 | 9.99 | 1.02 | 0.93 |
| ATAB | 12.55 | 0.75 | 10.27 | 0.29 | 0.99 |
| M12_51/49 | 5.16 | 0.43 | 10.68 | 0.28 | 0.98 |
| M13_35/65 | 6.90 | 1.04 | 10.98 | 0.53 | 0.93 |
| M23_34/66 | 9.83 | 2.27 | 11.17 | 1.04 | 0.85 |
| M123_26/25/48 | 7.49 | 0.67 | 10.72 | 0.35 | 0.98 |
| M123_15/58/27 | 9.80 | 1.08 | 9.42 | 0.61 | 0.97 |
| M123_11/10/79 | 11.10 | 0.79 | 9.75 | 0.36 | 0.98 |
| M123_59/14/27 | 3.85 | 0.55 | 11.92 | 0.33 | 0.95 |

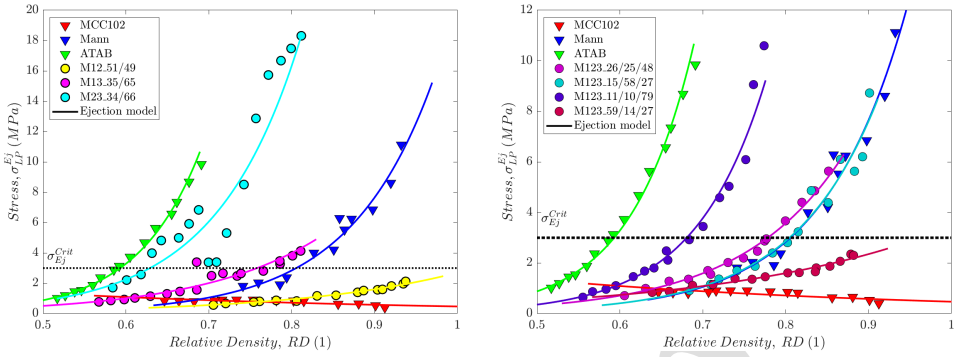


**(a)** Ejection stress vs. relative density of single component and binary mixtures




**(b)** Ejection stress vs. relative density of single component and ternary mixtures

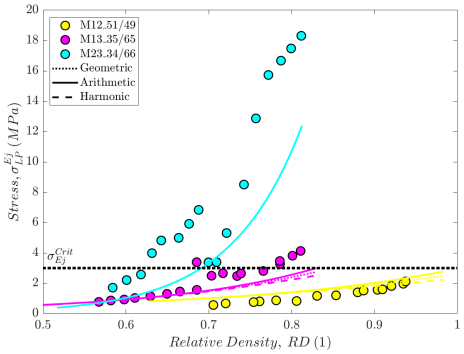


**(c)** Ejection stress vs. relative density of binary mixtures

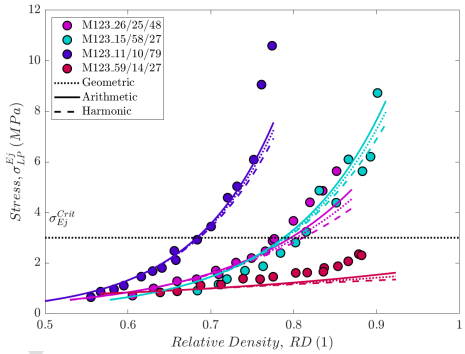


**(d)** Ejection stress vs. relative density of ternary mixtures

**Figure 8:** Ejection stress

## 7. SFW for single materials and binary and ternary mixtures

Formulations that satisfy the prescribed tablet requirements listed in Table 1 can be designed empirically by preparing and characterising mixtures of different compositions. To minimize the experimental space, we propose the concept of SFW (Successful Formulation Window), a tool that uses the rules of mixtures to predict the behaviour of various compositions. The SFW identifies the compaction pressure or relative density window where a given powder formulation meets the prescribed tablet requirements using the properties of the pure components as inputs.

### *7.1. Work-flow scheme*

The algorithm proposed to establish the SFW is shown schematically in Figure 9 where the inputs consist of the compaction simulator data (blue dashed box) and diametrical compression test data (orange dashed box). The red dashed box represents the formulation criteria (Table 1). The flow chart is implemented into a MATLAB routine used for data analysis and visualization (dashed black box).

The steps of the work-flow scheme are:

1. Generate experimental data using a compaction simulator, record tablet dimensions and material properties such as material bulk and true density and perform diametrical compression tests. Select the limit values for the design space (default values in Table 1).

2. Obtain relative density as a function of compaction pressure, and ejection stress and diametrical tensile strength as functions of relative density using the data analysis procedure described in Section 6 above.
3. Determine the lower boundary of the SFW to satisfy the minimum tablet strength criterion using tensile strength - relative density equation.
4. Calculate maximum admissible ejection stress using ejection stress - relative density relation and compaction pressure using compaction pressure - relative density relation. The lower value represents the upper boundary of the SFW.
5. Visualization of SFW.

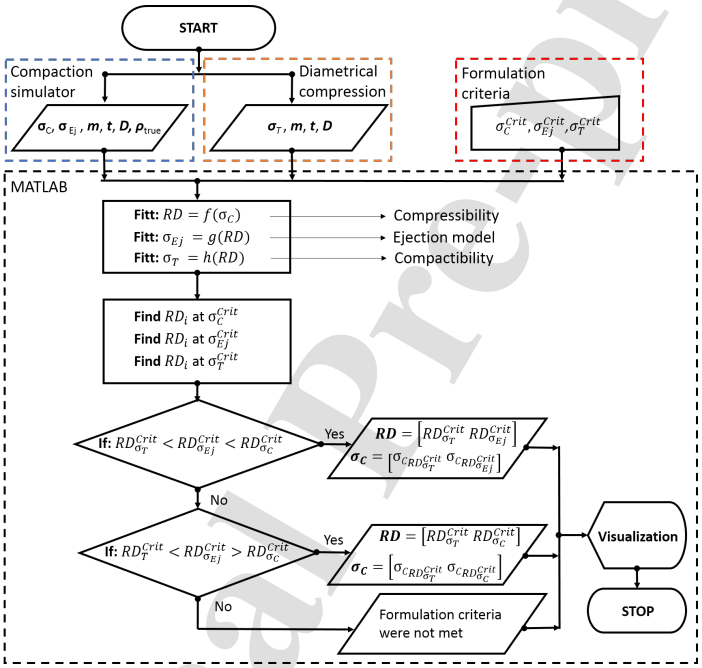


**Figure 9:** Flowchart of determining the SFW.

*7.2. Conditional space*

The measured mechanical properties including tablet strength and ejection stress define a conditional space for formulation requirements. Since tablet strength has the same unit as ejection stress ($MPa$), they can be plotted on a common axis (Strength and Stress). The conditional spaces for pure excipients are presented in Figure 10, where the black $x$ axis represents relative density and the orange $x$ axis represents compaction pressure. The $y$ axis is common for tensile strength and ejection stress. The black and green curves represent tensile strength and ejection stress, respectively. The SFW (magenta rectangle) is bounded on the relative density axis (the $x$ axis) by the minimum density requirement and the maximum compaction pressure (both prescribed in Table 1) which may limit the maximum achievable density. On the $y$ axis the SFW is situated between the minimum tensile strength and the maximum ejection stress (both prescribed in Table 1). SFWs exist when the minimum tensile strength is reached while ejection stress and compaction pressure are not exceeded. Figure 10 shows that while MCC presents a SFW, Mannitol and ATAB cannot be compressed into tablets that satisfy the requirements (Table 1). It is noted that in practice tablets can be made from these materials, but not within the constraints listed in Table 1.

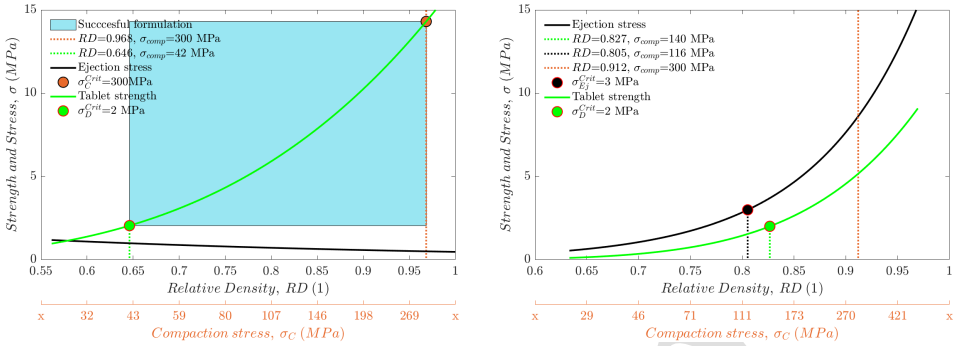


**(a)** MCC102. **(b)** Mann.

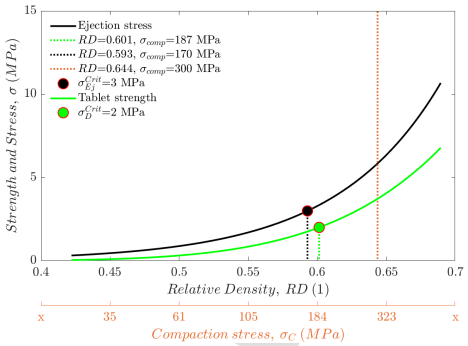


**(c)** ATAB.

**Figure 10:** Conditional space for minimum formulation requirements of pure excipients.

The conditional space for MCC102 shown in Figure 10a is bordered by strength criteria as minimum at compaction pressure 42 $MPa$ and relative density 0.646 and compaction pressure limit of 300 $MPa$ which gives a maximum at relative density 0.968, which approaches unity. Mann achieves the minimum tensile strength at compaction pressure 140 $MPa$ (or a relative density of 0.827) as shown in Figure 10b, however, the maximum allowed ejection stress is exceeded above a compaction pressure of 116 $MPa$ (a relative density 0.806). As such the SFW criteria were not met for pure Mannitol. Similarly, ATAB does not present a SFW as shown in Figure 10c because the ejection stress limit was reached at 170 $MPa$ (relative density of 0.593) before the tablet attained the minimum required strength (the minimum strength required a compaction pressure of 187 $MPa$, relative density of 0.601).

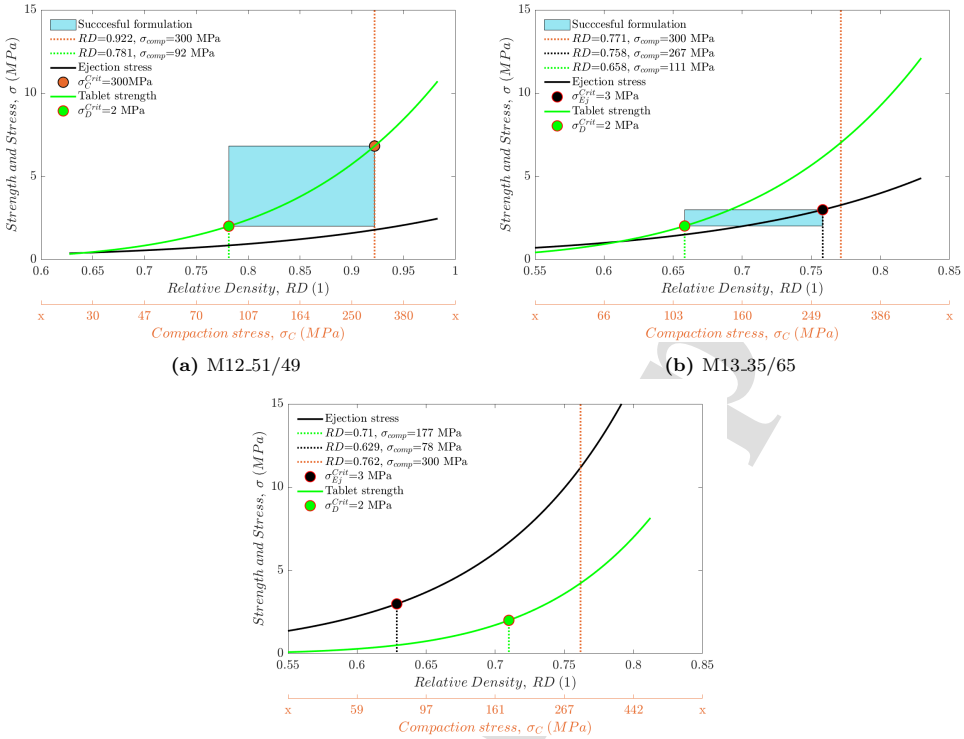


**(a)** M12_51/49 **(b)** M13_35/65

**(c)** M23_34/66

**Figure 11:** Conditional space for minimum formulation requirements of binary mixtures

Figure 11 presents the conditional space for binary mixtures with mass fractions listed in Table 4. MCC102 mixed with ATAB or Mann present SFWs, however the Mann - ATAB mixture does not. For M12_51/49 , Figure 11a, a lower bound of the SFW reached at a compaction pressure 92 $MPa$ (relative density of 0.781) and the higher bound was provided by the maximum compaction pressure criterion (at a relative density of 0.922). For M13_35/65 (Figure 11b) the lower boundary of the SFW was reached at 111 $MPa$ of compaction pressure (relative density 0.658) and the higher boundary of SFW was limited by the ejection stress at 267 $MPa$ of compaction pressure (relative density 0.758). Adding MCC102 into ATAB and ATAB decreased the ejection stress and increased compressibility and compactability. Figure 11c shows that M23_34/66 did not satisfy the minimum formulation requirements, which is not surprising because the minimum formulation requirements were not satisfied by any of the pure constituents.

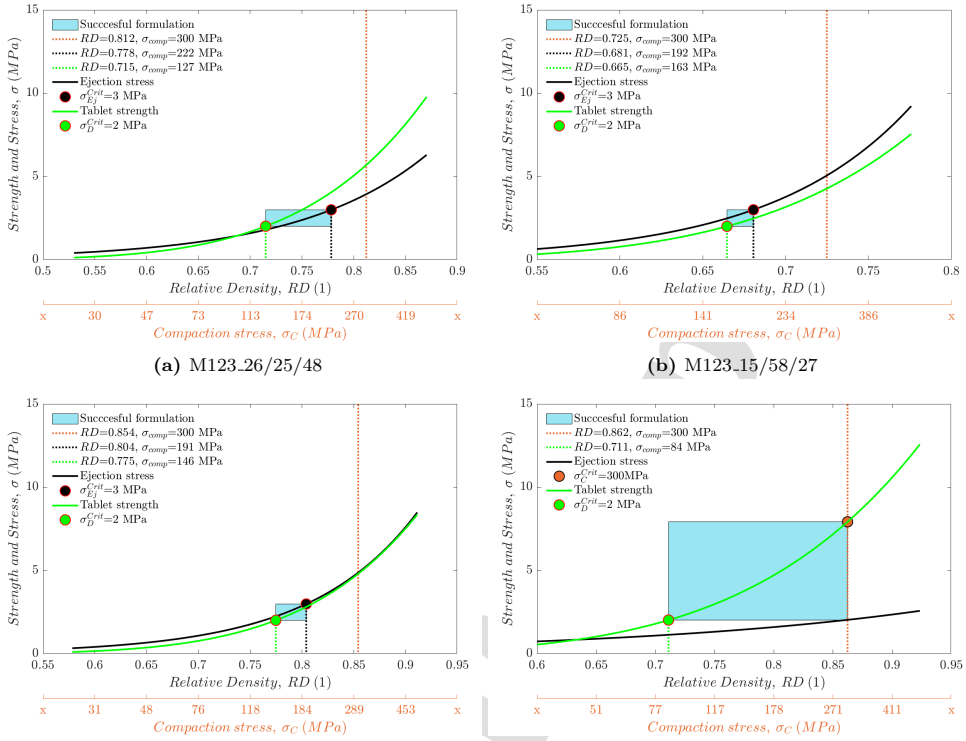


**(a)** M123_26/25/48 **(b)** M123_15/58/27

**(c)** M123_11/10/79 **(d)** M123_59/14/27

**Figure 12:** Conditional space for minimum formulation requirements of ternary mixtures

SFWs were possible for all four ternary mixtures as presented in Figure 12. The addition of a highly compressible and compactible MCC102 resulted in SFWs for other excipients that in pure form could not be pressed into tablets within the limiting criteria set in Table 1. Due to the simplicity of the compressibility, compactability and ejection stress models used, explicit equations for the upper and lower boundaries of the SFWs can be determined. The analytical expression for the lower boundary (see Table 10) was obtained by combining the compressibility equation from Table 2 with compactability equation from Table 3 and the prescribed formulation criteria from Table 1. Explicit solutions of compaction pressure needed to reach upper limit of SFWs ruled by ejection stress are presented in Table 11 together with the corresponding compressibility models. These equations can easily be programmed for practical use.

**Table 10:** Explicit expression of compaction pressure $\sigma_C$ at lower boundary of SFW

| *Compressibility* | *Compactability* | $\sigma_C$ | *No.* |
|---|---|---|---|
| Heckel: | *Ryshkewitch-Duckworth:* | $-\Big(A+log(-log(\sigma_{Dia}^{Crit}/\overline{\sigma}_{Dia})/e)\Big)/K$ | (19) |
| | *3 par. Power law:* | $-\Big(A+log(1-(\sigma_{Dia}^{Crit}/c)^{(1/n)}-RD_0)\Big)/K$ | (20) |
| Kawakita: | *Ryshkewitch-Duckworth:* | $-1/\Big(b+((e+log(\sigma_{Dia}^{Crit}/\overline{\sigma}_{Dia}))/e-1)/(RD_0b(a-1))\Big)$ | (21) |
| | *3 par. Power law:* | $-1/\Big(b+(RD_0+(\sigma_{Dia}^{Crit}/c)^{(1/n)}-1)/(RD_0b(a-1))\Big)$ | (22) |
| Kuentz-Leuenberger: | *Ryshkewitch-Duckworth:* | $\Big(RD_c+log(((e+log(\sigma_{Dia}^{Crit}/\overline{\sigma}_{Dia}))/e-1)/(RD_c-1))(RD_c-1)-(e+log(\sigma_{Dia}^{Crit}/\overline{\sigma}_{Dia}))/e\Big)/C$ | (23) |
| | *3 par. Power law:* | $-\Big(RD_0-RD_c-log((RD_0+(\sigma_{Dia}^{Crit}/c)^{(1/n)}-1)/(RD_c-1))(RD_c-1)+(\sigma_{Dia}^{Crit}/c)^{(1/n)}\Big)/C$ | (24) |
| Modified Gurnham: | *Ryshkewitch-Duckworth:* | $\overline{\sigma}_C\Big(\sigma_{Dia}^{Crit}/\overline{\sigma}_{Dia}\Big)^{(d/e)}$ | (25) |
| | *3 par. Power law:* | $\overline{\sigma}_C\,exp\Big(d(RD_0+(\sigma_{Dia}^{Crit}/c)^{(1/n)}-1)\Big)$ | (26) |

**Table 11:** Explicit expression of compaction pressure $\sigma_C$ at upper boundary of SFW

| *Compressibility* | $\sigma_C$ | *No* |
|---|---|---|
| Heckel: | $-\Big(A+log((\alpha+\beta-log(\sigma_{Ej}^{Crit})-RD_0\alpha)/\alpha)\Big)/K$ | (27) |
| Kawakita: | $-1/\Big(b+((log(\sigma_{Ej}^{Crit})-\beta+RD_0\alpha)/\alpha-1)/(RD_0b(a-1))\Big)$ | (28) |
| Kuentz-Leuenberger: | $\Big(RD_c-(log(\sigma_{Ej}^{Crit})-\beta+RD_0\alpha)/\alpha+log(((log(\sigma_{Ej}^{Crit})-\beta+RD_0\alpha)/\alpha-1)/(RD_c-1))(RD_c-1)\Big)/C$ | (29) |
| Modified Gurnham: | $\overline{\sigma}_C\,exp\Big(-(d(\alpha+\beta-log(\sigma_{Ej}^{Crit})-RD_0\alpha))/\alpha\Big)$ | (30) |

### *7.3. Evaluation of rules of mixtures*

In this section we evaluate averaging methods (geometric, arithmetic and harmonic) that could be used to predict the properties of mixtures (compressibility, compactability and ejection stress) using the properties of constituent materials. The predictions are compared with the actual experimental data for mixtures which are presented using black rectangles in the SFWs drawn in Figure 13.

Blank spaces (e.g. Mann, ATAB and M23_34/66 ) indicate that the conditions necessary for SFWs were not met. The lower limits of the formulation windows in compaction space (Figure 13a) and relative density space (Figure 13b) show good agreement with experimental data using geometrical averaging of the individual constituents in the mixture. The error (%) between the experimental data and the predictions based on the three rules of mixtures is presented in Figures 14a and 14b. It can be seen that the geometrical mean yields the lowest prediction error for the lower limits of the SFWs for all mixtures. The arithmetic mean overestimates the lower limits for all mixtures (bars above a 0% line). In contrast, the harmonic mean underestimates the lower limit for all mixtures (see bars below the horizontal axes in Figure 14a). The upper limits of SFWs were reached by the maximum compaction pressure criteria for M12_51/49, M23_34/66 and M123_26/25/48 for experimental as well as for theoretical prediction, hence the prediction error is 0%. The experimental upper limit of M13_35/65, M123_15/58/27, M123_11/10/79 and M123_59/14/27 is governed

by the ejection stress (illustrated on Figure 13a as the bars do not reach the compaction pressure limit). In the case of M13_35/65, the ejection criterion is reached at compaction pressure of 267 $MPa$, however the Pythagorean means predicted that the upper limit of SFW was imposed by the compaction pressure criterion as shown in Figure 13a, which gives prediction error of approximately 12%. The rules of mixtures overestimates the upper limit for M13_35/65, M123_26/25/48 and M123_11/10/79 and underestimates for M123_15/58/27. Further validation for other mixtures with various mass fractions is needed to establish the most suitable mean for predicting the SFWs.

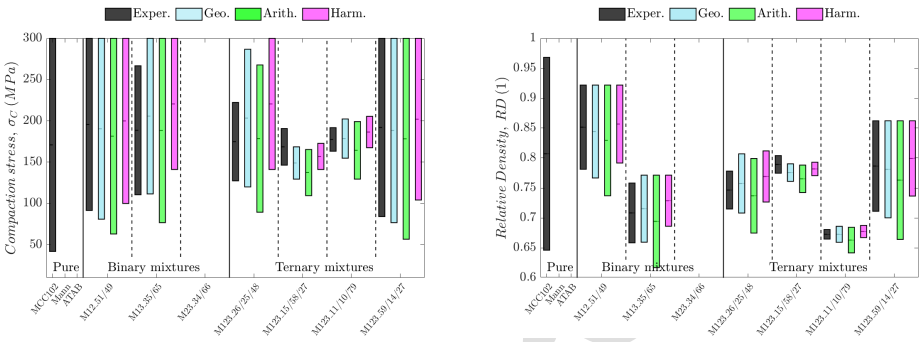


**(a)** Formulation space for compaction pressure **(b)** Formulation space for relative density

**Figure 13:** Successful Formulation Windows

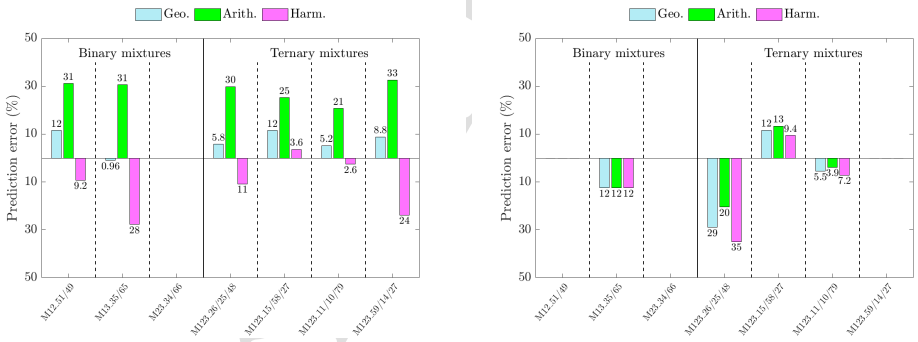


**(a)** Prediction error of lower criterion **(b)** Prediction error of upper criterion

**Figure 14:** SFW prediction error of various means

### *7.4. Ternary SFW*

Ternary contour plots of tablet strength and ejection stress with respect to volume fraction of constituents and compaction pressure are presented in Figures 15a and 15b, respectively. The interpretation of such contour plots is exemplified using the ejection stress behaviour presented in Figure 15b as follows. Consider a ternary mixture where the desired volume fraction of Mann is 0.4. First a horizontal line is drawn to the desired ejection stress. The exact volume fraction of ATAB and MCC102 (0.3 and 0.3 respectively) are obtained by projecting clockwise to the respective 120◦ and 240◦ axes. Note that the sum of the volume fractions must be to equal 1. As a general trend, Figures 15a and 15b show that the tablet strength increases,

and the ejection stress decreases by decreasing volume fraction of Mann and ATAB in the mixture. For example, a tablet made from pure Mann gains a strength of $4 MPa$ at compaction pressure approx. $250 MPa$ - point labelled "1" in Figure 15a, where the dash-dotted lines help visualize the compaction pressure at point 1. As another example, consider a tablet made of pure MCC102 which has a strength of $4\ MPa$ at compaction pressure approx. $70\ MPa$ - point labelled as "2". Following the $4\ MPa$ tablet strength contour it can be seen that a tablet made of pure ATAB does not reach this value in the compaction pressure range $50 - 300\ MPa$. Considering a binary mixture of ATAB and Mann , a tablet strength of $4\ MPa$ (point labelled "3") can be reached at compaction pressure of $300\ MPa$ with volume fractions of 0.75 and 0.25, respectively. Binary mixtures of ATAB and MCC102 will reach a strength of $4\ MPa$ approx. at a compaction pressure of $65\ MPa$ with volume fractions of 0.96 and 0.04, respectively at point "4".

Representing the results in a 5-dimensional space (3 compositions, compaction pressure and ejection stress or tablet strength) is less straight forward. An SFW of a mixture of three constituents is presented in Figure 15c. This visualization form shows a formulation window between a lower limit (green surface) and upper limit (black surface) reached at fractional composition of individual constituent at the corresponding compaction pressure. The fractional composition - compaction pressure space is divided into an SFW volume highlighted by soft blue colour and the transparent volume behind the limiting surfaces, where formulation criteria were not met. Such visualizations may serve as a tool to design the optimal formulation based on individual contribution of constituent property in a volume fraction - compaction pressure space. The visualization of SFW in fractional composition - compaction pressure space can be extended for more than three constituents.

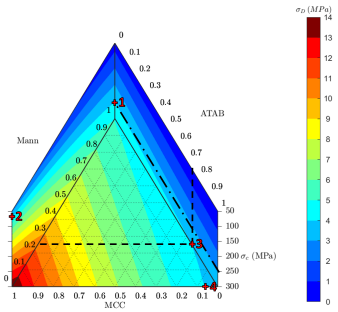


**(a)** Ternary contour of tablet strength.

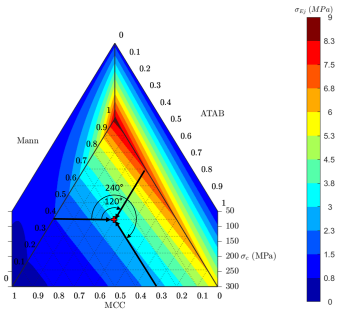


**(b)** Ternary contour of ejection stress.

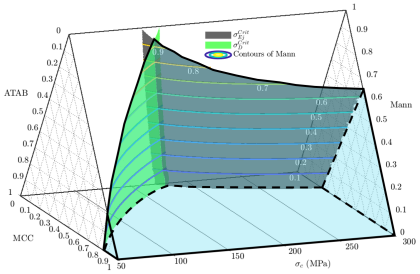


**(c)** Ternary plot of the formulation window.

**Figure 15:** Ternary contour with respect to the compaction pressure.

## 8. SFWs for lubricated materials

In this section we explore if the concept of SFWs could be extended to lubricated materials by examining the specific case of Mannitol - Magnesium stearate mixtures.

It is important to note that there is a small difference between the data for Mannitol presented in this section (labelled as Mann_0%) and Mannitol in the previous section (labelled as Mann). Here, Mann_0% compacts were manufactured using MTS 810 Material Test System (MTS, USA) as opposed to the Mann, which was compressed using a compaction simulator (ESH, Phoenix, Rubery Owen, Telford, England), under slightly different conditions e.g. environmental temperature and humidity during storage and manufacturing. The powder material was from the same batch. However, because of differences, in order to analyse the lubricated formulations manufactured using MTS, the data for Mann_0% is used for consistency.

### *8.1. Experimental data analysis for lubricated materials*

The compressibility and compactability data were fitted using the relationships presented in Section 6. Geometric, arithmetic and harmonic averaging were used in the compressibility-based rule of mixture to determine the properties of lubricated mixtures. The compressibility data of pure Mannitol (labelled Mann_0%) and pure MgSt are presented on Figure 16a with fully coloured blue and brown triangles and the models are represented accordingly by coloured lines. Experimental results of Mann_05% and Mann_1% are plotted with coloured circle shaped markers and the curves represent fitting by using compressibility models. Figure 16b compares the three rules of mixtures. It can be seen that for a relatively small amount of MgSt (0.5% and 1%) the difference between averaging methods is negligible. The parameters of compressibility models for Mann_0% , MgSt and their mixtures characterised experimentally are listed in Table 12. These results were used as a reference for validation of the SFWs of the mixtures determined. The coefficient of determination in Table 12 shows excellent accuracy of fitting models except for pure MgSt where the results present scatter throughout the compaction pressure range.

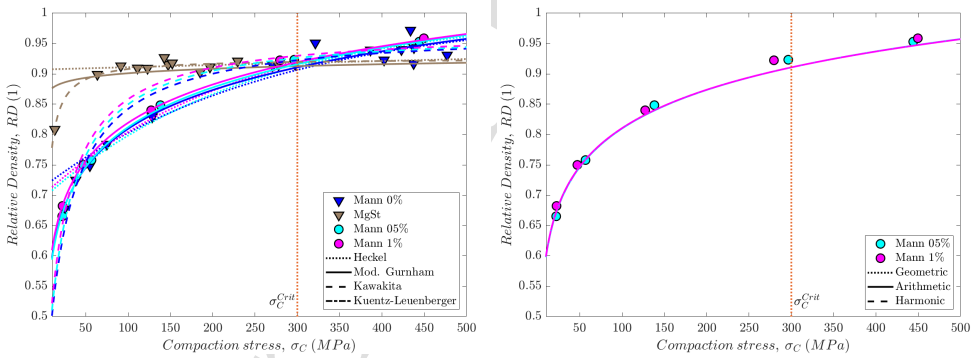


**(a)** Compressibility **(b)** Compressibility using various means

**Figure 16:** Compressibility of lubricated Mannitol

**Table 12:** Parameters of compressibility models and errors for lubricated Mannitol

| *Material* | *modified Gurnham* | | | | | *Kawakita-Lude* | | | | |
|---|---|---|---|---|---|---|---|---|---|---|
| | $\overline{\sigma}_C$ $(MPa)$ | $\pm\, Ci$ $(MPa)$ | $d$ $(-)$ | $\pm\, Ci$ $(-)$ | $R^2$ $(-)$ | $a$ $(-)$ | $\pm\, Ci$ $(-)$ | $1/b$ $(MPa)$ | $\pm\, Ci$ $(MPa)$ | $R^2$ $(-)$ |
| Mann_0% | 898.57 | 152.28 | 10.69 | 1.02 | 0.97 | 0.68 | 0.01 | 8.13 | 1.29 | 0.96 |
| MgSt | 997461.72 | 14010372.28 | 91.81 | 144.65 | 0.43 | 0.84 | 0.00 | 0.35 | 0.05 | 0.94 |
| Mann_05% | 888.72 | 153.96 | 10.77 | 0.89 | 1.00 | 0.68 | 0.02 | 7.33 | 2.19 | 0.96 |
| Mann_1% | 916.89 | 142.83 | 11.24 | 0.80 | 1.00 | 0.68 | 0.02 | 6.75 | 2.10 | 0.95 |
| | *Kuentz-Leuenberger* | | | | | *Heckel* | | | | |
| | $1/C$ $(MPa)$ | $\pm\, Ci$ $(MPa)$ | $RD_c$ $(-)$ | $\pm\, Ci$ $(-)$ | $R^2$ $(-)$ | $1/K$ $(MPa)$ | $\pm\, Ci$ $(MPa)$ | $A$ $(-)$ | $\pm\, Ci$ $(-)$ | $R^2$ $(-)$ |
| Mann_0% | 629.37 | 582.84 | 0.57 | 0.29 | 0.85 | 313.81 | 59.12 | 1.22 | 0.26 | 0.87 |
| MgSt | 1121.16 | 3943.13 | 0.29 | 0.44 | 0.31 | 3185.92 | 2334.19 | 2.37 | 0.16 | 0.06 |
| Mann_05% | 1208.82 | 586.48 | 0.40 | 0.10 | 0.99 | 301.69 | 67.97 | 1.19 | 0.32 | 0.96 |
| Mann_1% | 1121.46 | 619.49 | 0.40 | 0.12 | 0.99 | 296.48 | 63.53 | 1.20 | 0.30 | 0.96 |

The compactability data for the excipient, the lubricant and their mixtures were fitted using the models listed in Table 3. The fitting parameters together with the coefficient of determination are listed in Table 13. The results of the fitting procedure are visualised in Figure 17a. It can be seen that differences in the fitting are very small. The 3-parameter power law model fits data with higher precision (see the coefficient of determination in Table 13). The three mixture rules applied for the Gurnham model for compressibility and the 3-parameter power law for compactability are plotted in Figure 17b. Differences in compactability of the mixtures using various means are negligible due to small mass fraction of the lubricant in the mixture. It was noted that the compactability of mixtures lubricated with MgSt is strongly affected by mixing time (Kikuta and Kitamori, 1994), thus the data in Figure 17a are specific to the mixing conditions given in Section 5.1. To generalise this procedure the effect of mixing time should be incorporated into the 3-parameter power law compactability model through additional model parameters.

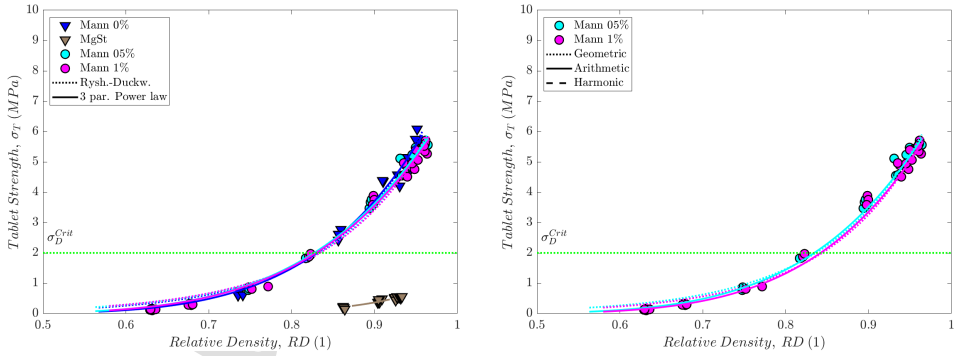


**(a)** Semi-log space of tablet strength vs. relative density of single component and binary mixtures

**(b)** Semi-log space of tablet strength vs. relative density of binary mixtures

**Figure 17:** Compactability of the tablet

**Table 13:** Parameters of compactability model (3 par. Power law) and errors for lubricated Mannitol

| *Material* | *Ryshkewitch-Duckworth* | | | | | *3 par. Power law* | | | | |
|---|---|---|---|---|---|---|---|---|---|---|
| | $\overline{\sigma}_{Dia}$ $(MPa)$ | $\pm\, Ci$ $(MPa)$ | $e$ $(-)$ | $\pm\, Ci$ $(-)$ | $R^2$ $(-)$ | $c$ $(MPa)$ | $\pm\, Ci$ $(MPa)$ | $n$ $(-)$ | $\pm\, Ci$ $(-)$ | $R^2$ $(-)$ |
| Mann_0% | 8.70 | 0.80 | 8.76 | 1.22 | 0.97 | 49.68 | 16.17 | 4.92 | 0.68 | 0.98 |
| MgSt | 1.38 | 0.27 | 13.28 | 2.39 | 0.91 | 6.29 | 2.87 | 10.08 | 1.78 | 0.91 |
| Mann_05% | 7.95 | 0.45 | 8.28 | 0.77 | 0.99 | 38.72 | 5.85 | 4.52 | 0.32 | 0.99 |
| Mann_1% | 7.72 | 0.41 | 8.14 | 0.75 | 0.99 | 37.81 | 5.79 | 4.55 | 0.33 | 0.99 |

Experimental ejection stress data for Mann_0%, MgSt, Mann_05% and Mann_1% are plotted with markers in Figure 18a together with the ejection model Equation (7). The fitting parameters and coefficient of determination are listed in Table 14. The fittings for mixtures are used as reference data for predictive model validation. The coefficient of determination of MgSt acquires value of 0.00 due to the ability of material to form a compact only in a very limited range and the results being scattered in this range. Moreover, the negative value of $\alpha$ in Table 14 means slightly decreasing trend of ejection stress with increasing relative density of the compact indicates means that the kinetic friction between tablet and wall during ejection decreases for tablet compacted under higher pressure.

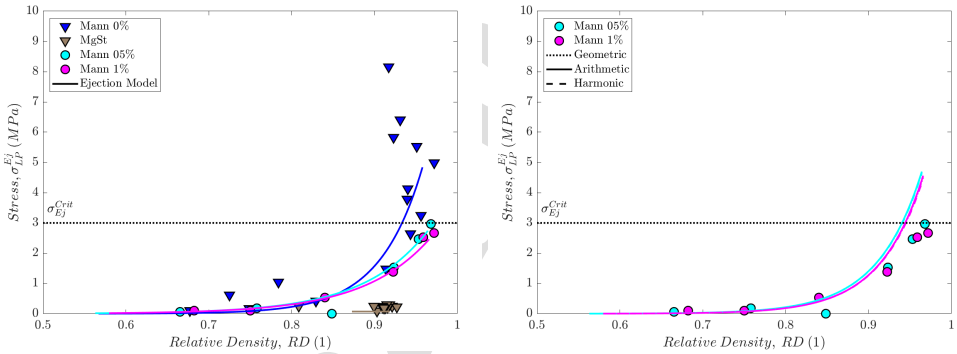


**(a)** Ejection stress vs. relative density **(b)** Ejection stress vs. relative density

**Figure 18:** Semi-log space of lubricated Mannitol ejection stress

**Table 14:** Parameters of ejection model and errors for lubricated Mannitol

| *Material* | $\alpha$ | $Ci$ | $\beta$ | $Ci$ | $R^2$ |
|---|---|---|---|---|---|
| | $(Pa)$ | $\pm$ | $(Pa)$ | $\pm$ | $(-)$ |
| Mann_0% | 13.07 | 3.68 | 7.21 | 2.06 | 0.82 |
| MgSt | -0.34 | 7.25 | 12.56 | 5.50 | 0.00 |
| Mann_05% | 13.27 | 0.98 | 6.37 | 0.53 | 1.00 |
| Mann_1% | 12.79 | 3.44 | 6.52 | 1.87 | 0.96 |

*8.2. Conditional space for lubricated material*

The SFWs satisfying the minimum formulation requirements for the pure excipient, lubricant and their mixtures was determined using the compressibility, compactability and ejection stress models obtained by fitting of experimental data are plotted in conditional space in Figures 19 and 20. The SFW in conditional space for pure Mann_0% (the cyan blue rectangle in Figure 19a) is limited by the minimum tablet strength criterion at the compaction pressure of 126 $MPa$ with relative density of 0.831 and the maximum compaction pressure criterion 300 $MPa$ with relative density of 0.916. The compaction pressure limit closely approaches the ejection stress limit. A direct comparison of the Mann_0% Figure 19a and Mann Figure 10b (which were obtained under slightly different conditions as discussed above) shows that while Mann does not present a SFW due to reaching the ejection stress limit at a compaction pressure level where the required tablet strength is not yet achieved, Mann_0% presents a SFW. Satisfying the prescribed criteria for Mann_0% is due to significantly lower ejection stress which can be attributed to the different lubrication method of the die and punches during tablet compaction. Minimum formulation requirements for pure MgSt were not met, and so a SFW in conditional space (cyan blue coloured rectangle) was not formed as shown in Figure 19b. The reason is that tablet strength criterion was not reached before the compaction pressure limit. Lubricated Mannitol with 0.5% of MgSt (Figure 19a) reached the tablet strength criterion at 117 $MPa$ with a relative density of 0.827. The upper limit of SFW was provided by the maximum compaction stress limit at 0.916 relative density. The compaction pressure needed to reach the minimum tablet strength of Mann_1% (Figure 19b) was 112 $MPa$ with relative density of 0.830 and upper limit of SFW was determined by the compaction pressure limit at 0.919 relative density. As expected, the compaction model indicated that increasing the lubricant mass fraction resulted in an increase of compaction pressure necessary to reach the lower limit of SFW.

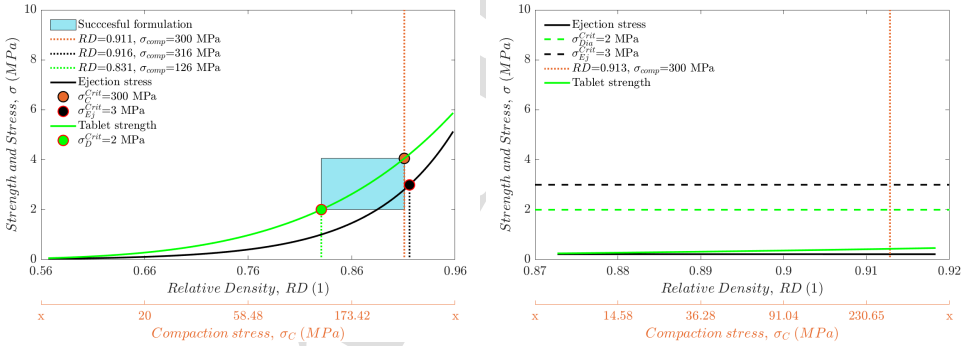


**(a)** Mann_0% **(b)** MgSt

**Figure 19:** Conditional space for minimum formulation requirements of pure Mannitol and Magnesium Stearate

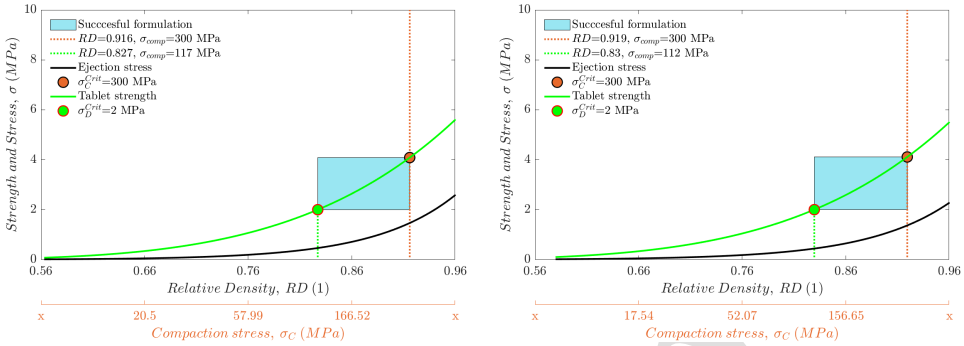


**(a)** Mann_05%. **(b)** Mann_1%.

**Figure 20:** Conditional space for minimum formulation requirements of lubricated Mannitol.

### *8.3. Evaluation of rules of mixture for lubricated powders*

Evaluation of averaging methods for SFW in compaction space and relative density space are presented in Figures 21a and 21b, respectively. The black rectangle represents experimental results and coloured rectangle represents averaging method as indicated in the legend. As described in detail in Section 8.1 the differences between the averaging methods are small due to small mass fraction of the lubricant. A quantitative comparison of averaging methods is presented in Figure 22. It can be seen that in case of lubricated material arithmetic mean presents the lowest prediction error of 7.6% for Mann_05% and 13% for Mann_1% in compaction space. The minimum requirements for MgSt were not met (see blank space in Figures 21a and 21b). By comparing the SFWs of lubricated materials it can be seen that the use of the compressibility based mixture rule and any of the three averaging methods is valid also for the case where the second constituent was a lubricant with very low volume fraction. This work covered a relatively narrow lubricant content, however this is typical to pharmaceutical formulations. A wider range of lubricant volume fraction may provide further understanding of how the lubricant influences the upper and lower limit of SFWs with additional volume fraction of a third constituent.

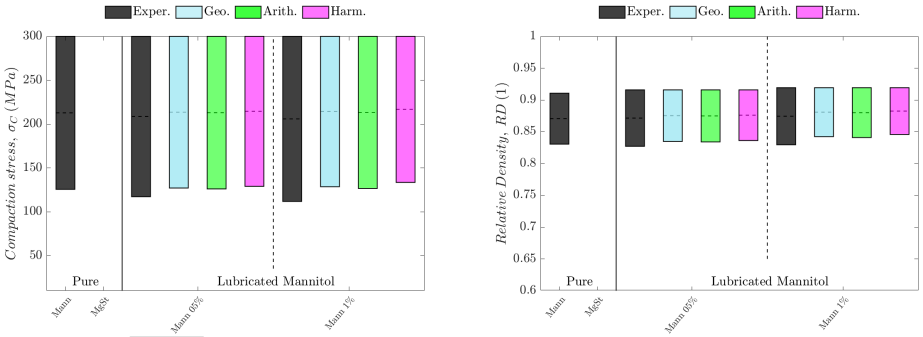


**(a)** Formulation space for compaction pressure **(b)** Formulation space for relative density

**Figure 21:** Formulation windows of lubricated Mannitol

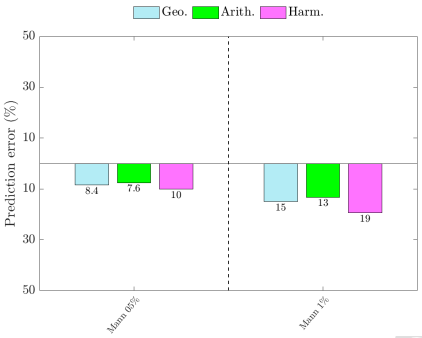


**Figure 22:** Prediction error of lower criterion of lubricated material

## 9. Conclusions

An algorithm was proposed to determine Successful Formulation Windows (SFWs), which provide the compaction pressure and porosity range where a given formulation can be compressed into a tablet that satisfies a set of mechanical quality attributes (minimum tensile strength, maximum compaction pressure, and maximum ejection stress). The method was developed and validated for single materials, binary and ternary mixtures and mixtures containing lubricant. The three quality attributes for mixtures were determined using rules of mixture based on the volume fraction of an individual component under the same compaction pressure. Arithmetic, geometric and harmonic means were evaluated, and the geometric averaging was found to provide the best correlation with the experimental data. The selected powders are representative and widely used pharmaceutical excipients that cover deformation mechanisms under compaction ranging from plastic deformation (microcrystalline cellulose) to brittle behaviour (calcium phosphate). Based on the lubricated material systems considered in this work it is interesting to conclude that the mixing rules were applicable to low lubricant content (0.55-1% w/w); perhaps due to the fact that the lubricant is made of very fine particle that adequately cover larger particles and in this respect the lubricant percolates.

A mechanistic prediction of tablet quality attributes based on the properties of the constituent particles is desirable, however, until such models mature, the empirically based SFW method introduced above represents a practical tool for the design of binary and ternary formulations as well as lubricated materials. Subject to validation, the SFWs methodology can be extended to other tablet quality criteria, for example: disintegration time, dissolution time, friability, minimum and maximum relative density, maximum residual radial stress etc.

## Acknowledgement

Peter Polak is grateful to AstraZeneca, Macclesfield for financial support for PhD research, material and use of the facilities. The SFW algorithm was programmed into a toolkit part of the "Virtual Formulation Laboratory for prediction and optimisation of manufacturability of advanced solids based formulations" project funded by the UK Engineering and Physical Science Research Council (reference EP/N025261/1).

## References

Al-Sabbagh, M., Polak, P., Roberts, R., Reynolds, G., and Sinka, I. (2018). Methodology to estimate the break force of pharmaceutical tablets with curved faces under diametrical compression. *International journal of pharmaceutics*.

Arndt, O.-R. and Kleinebudde, P. (2018). Influence of binder properties on dry granules and tablets. *Powder Technology*, 337:68–77.

Balshin, M. Y. (1949). Relation of mechanical properties of powder metals and their porosity and the ultimate properties of porous metal-ceramic materials. In *Dokl Akad Nauk SSSR*, volume 67, pages 831–834.

Bangudu, A. and Pilpel, N. (1984). Tensile strengths of paracetamol and avicel powders and their mixtures. *Journal of pharmacy and pharmacology*, 36(11):717–722.

Bolhuis, G. K. and Anthony Armstrong, N. (2006). Excipients for direct compactionan update. *Pharmaceutical development and technology*, 11(1):111–124.

Bos, C., Vromans, H., and Lerk, C. (1991). Lubricant sensitivity in relation to bulk density for granulations based on starch or cellulose. *International journal of pharmaceutics*, 67(1):39–49.

Bowden, F. P. and Tabor, D. (1967). Friction and lubrification.

Brewin, P. R., Coube, O., Doremus, P., and Tweed, J. H. (2007). *Modelling of powder die compaction*. Springer Science & Business Media.

Busignies, V., Leclerc, B., Porion, P., Evesque, P., Couarraze, G., and Tchoreloff, P. (2006). Compaction behaviour and new predictive approach to the compressibility of binary mixtures of pharmaceutical excipients. *European journal of pharmaceutics and biopharmaceutics*, 64(1):66–74.

Busignies, V., Mazel, V., Diarra, H., and Tchoreloff, P. (2012). Prediction of the compressibility of complex mixtures of pharmaceutical powders. *International journal of pharmaceutics*, 436(1-2):862–868.

Capece, M., Ho, R., Strong, J., and Gao, P. (2015). Prediction of powder flow performance using a multi-component granular bond number. *Powder Technology*, 286:561–571.

Cardei, Petru, G. I. (2017). A critical analysis of empirical formulas describing the phenomenon of compaction of the powders. *Modern Technology & Engineering*, 2(1):1–20.

Carneiro, F. and Barcellos, A. (1953). Résistance à la traction des bétons. *Bulletin Rilem*, 1(13):97–108.

Chan, S., Pilpel, N., and Cheng, D.-H. (1983). The tensile strengths of single powders and binary mixtures. *Powder Technology*, 34(2):173–189.

Cheng, D.-H. (1968). The tensile strength of powders. *Chemical Engineering Science*, 23(12):1405–1420.

Denny, P. (2002). Compaction equations: a comparison of the heckel and kawakita equations. *Powder Technology*, 127(2):162–172.

Doelker, E. (1993). Comparative compaction properties of various microcrystalline cellulose types and generic products. *Drug development and industrial pharmacy*, 19(17-18):2399–2471.

Doelker, E. and Massuelle, D. (2004). Benefits of die-wall instrumentation for research and development in tabletting. *European journal of pharmaceutics and biopharmaceutics*, 58(2):427–444.

Doremus, P., Toussaint, F., and Alvain, O. (2001). Simple tests and standard procedure for the characterisation of green compacted powder. *Nato Science Series Sub Series III Computer And Systems Sciences*, 176:29–41.

Etzler, F. M., Bramante, T., Deanne, R., Sienkiewicz, S., and Chen, F. (2011). Tablet tensile strength: an adhesion science perspective. *Journal of Adhesion Science and Technology*, 25(4-5):501–519.

Fell, J. and Newton, J. (1970). Determination of tablet strength by the diametral-compression test. *Journal of pharmaceutical sciences*, 59(5):688–691.

Fleck, N. (1995). A crystal plasticity view of powder compaction. *Acta metallurgica et materialia*, 43(8):3177–3184.

Garner, S., Strong, J., and Zavaliangos, A. (2015). The extrapolation of the drucker–prager/cap material parameters to low and high relative densities. *Powder Technology*, 283:210–226.

Gurnham, C. F. and Masson, H. J. (1946). Expression of liquids from fibrous materials. *Industrial & Engineering Chemistry*, 38(12):1309–1315.

Hasselman, D. (1969). Griffith flaws and the effect of porosity on tensile strength of brittle ceramics. *Journal of the American Ceramic Society*, 52(8):457–457.

Heckel, R. (1961a). Density-pressure relationships in powder compaction. *Trans Metall Soc AIME*, 221(4):671–675.

Heckel, W. (1961b). An analysis of powder compaction phenomena. *Trans. Metall. Soc. AIME*, 221:671–675.

Higuchi, T., Elowe, L., and Busse, L. (1954). The physics of tablet compression. v. studies on aspirin, lactose, lactose-aspirin, and sulfadiazine tablets. *Journal of the American Pharmaceutical Association*, 43(11):685–689.

Hoag, S. W., Dave, V. S., and Moolchandani, V. (2008). Compression and compaction. In *Pharmaceutical Dosage Forms-Tablets*, pages 571–646. CRC Press.

Hwang, R.-c. and Peck, G. R. (2001). Compression and tablet characteristics of various types of lactose and dibasic calcium phosphate. *Pharmaceutical technology*.

Jarosz, P. J. and Parrott, E. L. (1984). Effect of lubricants on tensile strengths of tablets. *Drug Development and Industrial Pharmacy*, 10(2):259–273.

Juban, A., Nouguier-Lehon, C., Briancon, S., Hoc, T., and Puel, F. (2015). Predictive model for tensile strength of pharmaceutical tablets based on local hardness measurements. *International journal of pharmaceutics*, 490(1-2):438–445.

Kawakita, K. and Lüdde, K.-H. (1971). Some considerations on powder compression equations. *Powder technology*, 4(2):61–68.

Kikuta, J.-I. and Kitamori, N. (1994). Effect of mixing time on the lubricating properties of magnesium stearate and the final characteristics of the compressed tablets. *Drug development and industrial pharmacy*, 20(3):343–355.

Kuentz, M. and Leuenberger, H. (1999). Pressure susceptibility of polymer tablets as a critical property: a modified heckel equation. *Journal of pharmaceutical sciences*, 88(2):174–179.

Kuentz, M. and Leuenberger, H. (2000). A new theoretical approach to tablet strength of a binary mixture consisting of a well and a poorly compactable substance. *European journal of pharmaceutics and biopharmaceutics*, 49(2):151–159.

Kuentz, M. T. (1999). *Mechanical Properties of Pharmaceutical Polymer Tablets-Modelling by Taking Into Account the Theory of Percolation*. PhD thesis, Verlag nicht ermittelbar.

LaMarche, K., Buckley, D., Hartley, R., Qian, F., and Badawy, S. (2014). Assessing materials' tablet compaction properties using the drucker–prager cap model. *Powder Technology*, 267:208–220.

Leane, M., Pitt, K., Reynolds, G., and Group, M. C. S. M. W. (2015). A proposal for a drug product manufacturing classification system (mcs) for oral solid dosage forms. *Pharmaceutical development and technology*, 20(1):12–21.

Leuenberger, H. (1982). The compressibility and compactibility of powder systems. *International Journal of Pharmaceutics*, 12(1):41–55.

Mahmoodi, F., Klevan, I., Nordström, J., Alderborn, G., and Frenning, G. (2013). A comparison between two powder compaction parameters of plasticity: The effective medium a parameter and the heckel 1/k parameter. *International journal of pharmaceutics*, 453(2):295–299.

Mellor, M. and Hawkes, I. (1971). Measurement of tensile strength by diametral compression of discs and annuli. *Engineering Geology*, 5(3):173–225.

Michrafy, A., Michrafy, M., Kadiri, M., and Dodds, J. (2007). Predictions of tensile strength of binary tablets using linear and power law mixing rules. *International journal of Pharmaceutics*, 333(1-2):118–126.

Miller, T. and York, P. (1988). Pharmaceutical tablet lubrication. *International journal of pharmaceutics*, 41(1-2):1–19.

Mitrevej, K. T. and Augsburger, L. (1982). Adhesion of tablets in a rotary tablet press ii. effects of blending time, running time, and lubricant concentration. *Drug Development and Industrial Pharmacy*, 8(2):237–282.

Patel, S., Kaushal, A. M., and Bansal, A. K. (2010). Mechanistic investigation on pressure dependency of heckel parameter. *International journal of pharmaceutics*, 389(1-2):66–73.

Paul, S. and Sun, C. C. (2017a). Lubrication with magnesium stearate increases tablet brittleness. *Powder Technology*, 309:126–132.

Paul, S. and Sun, C. C. (2017b). The suitability of common compressibility equations for characterizing plasticity of diverse powders. *International journal of pharmaceutics*, 532(1):124–130.

Paul, S. and Sun, C. C. (2018). Systematic evaluation of common lubricants for optimal use in tablet formulation. *European Journal of Pharmaceutical Sciences*, 117:118–127.

Persson, A.-S. and Alderborn, G. (2018). A hybrid approach to predict the relationship between tablet tensile strength and compaction pressure using analytical powder compression. *European Journal of Pharmaceutics and Biopharmaceutics*, 125:28–37.

Persson, A.-S., Nordström, J., Frenning, G., and Alderborn, G. (2016). Compression analysis for assessment of pellet plasticity: Identification of reactant pores and comparison between heckel, kawakita, and adams equations. *Chemical Engineering Research and Design*, 110:183–191.

Pifferi, G. and Restani, P. (2003). The safety of pharmaceutical excipients. *Il Farmaco*, 58(8):541–550.

Radojevic, J. and Zavaliangos, A. (2017). On the post-compaction evolution of tensile strength of sodium chloride-starch mixture tablets. *Journal of pharmaceutical sciences*, 106(8):2088–2096.

Ramirez, N., Melgoza, L. M., Kuentz, M., Sandoval, H., and Caraballo, I. (2004). Comparison of different mathematical models for the tensile strength–relative density profiles of binary tablets. *European journal of pharmaceutical sciences*, 22(1):19–23.

Reddy, K. V. R., Divakar, K., Venkateswara, B., and Reddy, P. (2013). Pharmaceutical excipients-their mechanisms. *RJPDFT*, 5(6):355–360.

Reynolds, G. K., Campbell, J. I., and Roberts, R. J. (2017). A compressibility based model for predicting the tensile strength of directly compressed pharmaceutical powder mixtures. *International journal of pharmaceutics*, 531(1):215–224.

Roberts, M., Ford, J. L., Rowe, P. H., Dyas, A. M., MacLeod, G. S., Fell, J. T., and Smith, G. W. (2004). Effect of lubricant type and concentration on the punch tip adherence of model ibuprofen formulations. *Journal of pharmacy and pharmacology*, 56(3):299–305.

Roblot-Treupel, L. and Puisieux, F. (1986). Distribution of magnesium stearate on the surface of lubricated particles. *International journal of pharmaceutics*, 31(1-2):131–136.

Rowe, R. and Roberts, R. (1995). 1 the mechanical properties of powders. In *Advances in pharmaceutical sciences*, volume 7, pages 1–IV. Elsevier.

Rumpf, H. (1962). Agglomeration, ed. wa knepper. *Interscience Pub., New York*, 379.

Ryshkewitch, E. (1953). Compression strength of porous sintered alumina and zirconia: 9th communication to ceramography. *Journal of the American Ceramic Society*, 36(2):65–68.

Schiller, K. (1971). Strength of porous materials. *Cement and Concrete Research*, 1(4):419–422.

Sheskey, J. P., Hancock, C. B., Moss, P. G., and Goldfarb, J. D. (2020). *Handbook of pharmaceutical excipients*. Pharmaceutical Press, 9th edition.

Shotton, E. and Ganderton, D. (1961). The strength of compressed tablets: Iii. the relation of particle size, bonding and capping in tablets of sodium chloride, aspirin and hexamine. *Journal of Pharmacy and Pharmacology*, 13(S1):144T–152T.

Shotton, E. and Lewis, C. (1964). Some observations on the effect of lubrication on the crushing strength of tablets. *Journal of Pharmacy and Pharmacology*, 16(S1):111T–120T.

Sinka, I., Cunningham, J., and Zavaliangos, A. (2001). Experimental characterization and numerical simulation of die wall friction in pharmaceutical powder compaction. *Advances in Powder Metallurgy and Particulate Materials*, (1):1–46.

Smalley, V. and Smalley, I. (1964). Tensile strength of granular materials. *Nature*, 202(4928):168.

Thoorens, G., Krier, F., Leclercq, B., Carlin, B., and Evrard, B. (2014). Microcrystalline cellulose, a direct compression binder in a quality by design environmenta review. *International Journal of Pharmaceutics*, 473(1-2):64–72.

Tye, C. K., Sun, C. C., and Amidon, G. E. (2005). Evaluation of the effects of tableting speed on the relationships between compaction pressure, tablet tensile strength, and tablet solid fraction. *Journal of pharmaceutical sciences*, 94(3):465–472.

Uzondu, B., Leung, L. Y., Mao, C., and Yang, C.-Y. (2018). A mechanistic study on tablet ejection force and its sensitivity to lubrication for pharmaceutical powders. *International journal of pharmaceutics*, 543(1):234–244.

Walker, E. (1923). The properties of powders. part vi. the compressibility of powders. *Transactions of the Faraday Society*, 19(July):73–82.

Wang, J., Wen, H., and Desai, D. (2010). Lubrication in tablet formulations. *European journal of pharmaceutics and biopharmaceutics*, 75(1):1–15.

Wu, C.-Y., Best, S. M., Bentham, A. C., Hancock, B. C., and Bonfield, W. (2005). A simple predictive model for the tensile strength of binary tablets. *European Journal of Pharmaceutical Sciences*, 25(2-3):331–336.

Wu, C.-Y., Best, S. M., Bentham, A. C., Hancock, B. C., and Bonfield, W. (2006). Predicting the tensile strength of compacted multi-component mixtures of pharmaceutical powders. *Pharmaceutical research*, 23(8):1898–1905.

Zhao, J., Burt, H., and Miller, R. (2006). The gurnham equation in characterizing the compressibility of pharmaceutical materials. *International journal of pharmaceutics*, 317(2):109–113.

Zuurman, K., Van der Voort Maarschalk, K., and Bolhuis, G. (1999). Effect of magnesium stearate on bonding and porosity expansion of tablets produced from materials with different consolidation properties. *International journal of pharmaceutics*, 179(1):107–115.

| Formulation criteria | Value |
|---|---|
| Tensile strength | Minimum 2 MPa |
| Ejection stress | Maximum 3 MPa |
| Compaction pressure | Maximum 300 MPa |

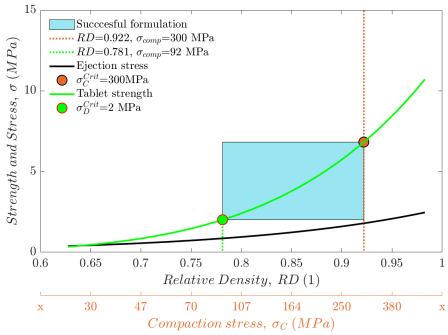


Conditional space for minimum formulation requirements of a binary mixture limited by minimum tensile strength and maximum compaction pressure

**Successful Formulation Window**

SFW: compaction pressure and density for single materials and mixtures

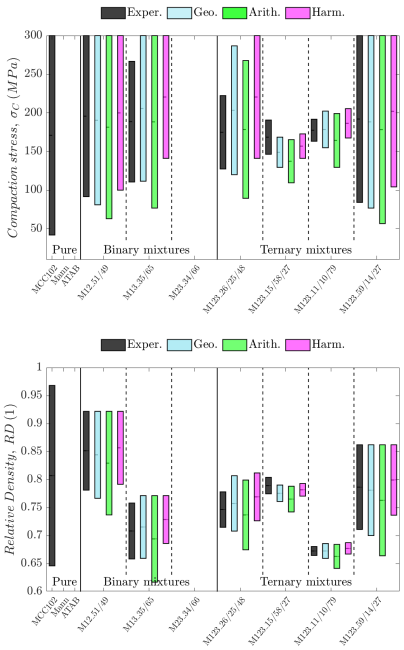


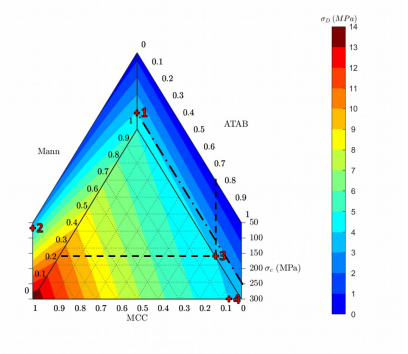


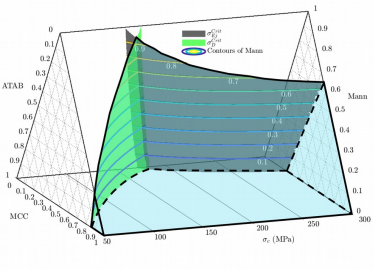


Ternary contour for tablet strength (top) and SFW

P. Polak: Conceptualization; Data curation; Formal analysis; Investigation; Methodology; Visualization; Roles/Writing - original draft

I.C. Sinka: Conceptualization, Funding acquisition; Investigation; Methodology; Project administration; Resources; Supervision; Writing - review & editing

G.K. Reynolds, R.J. Roberts: Conceptualization, Funding acquisition; Methodology; Resources; Writing - review & editing

**Declaration of interests**

☐ The authors declare that they have no known competing financial interests or personal relationships that could have appeared to influence the work reported in this paper.

☒ The authors declare the following financial interests/personal relationships which may be considered as potential competing interests:

I.C. Sinka reports financial support was provided by Engineering and Physical Sciences Research Council. P. Polak reports financial support was provided by AstraZeneca.